June 18, 2018 at International workshop for String theory, Gravitation and Cosmology, APCTP Pohang

Current status of gravitational wave detections and SOGRO

Gungwon Kang (KISTI)
and KKN Collaboration

Outline

I. Status on GW detections

- Summary of detection events
- Perspectives

II. Introduction to SOGRO

- Conceptual design
- Target sciences

On behalf of the KKN Collaboration

I. Status on GW detections

- First detection on Sept. 14, 2015 at 09:50:45 UTC: GW150914

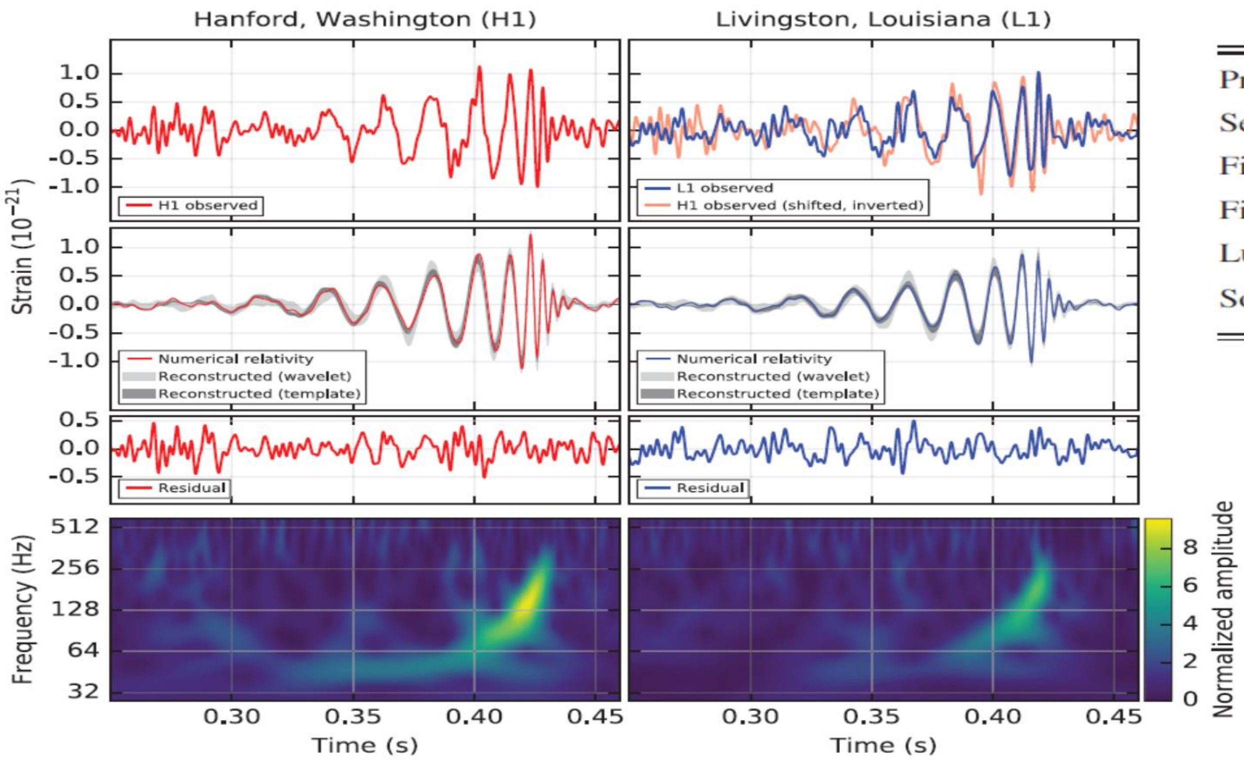

PRL **116**, 061102 (2016)

Primary black hole mass	$36^{+5}_{-4} M_\odot$
Secondary black hole mass	$29^{+4}_{-4} M_\odot$
Final black hole mass	$62^{+4}_{-4} M_\odot$
Final black hole spin	$0.67^{+0.05}_{-0.07}$
Luminosity distance	410^{+160}_{-180} Mpc
Source redshift z	$0.09^{+0.03}_{-0.04}$

- From a binary black hole coalesce
- SNR ~ 24, equivalent to a significance $\gtrsim 5.1\sigma$
- Agree with GR very well

✓ GW Events from O1 (2015/09/12~2016/01/12) & O2 (2016/11/30~2017/08/25):

- 4 BH mergers (GW150914, GW151226, GW170104, GW170814)
- 1 BH merger candidate (LVT151012)
- 1 NS merger (GW170817)

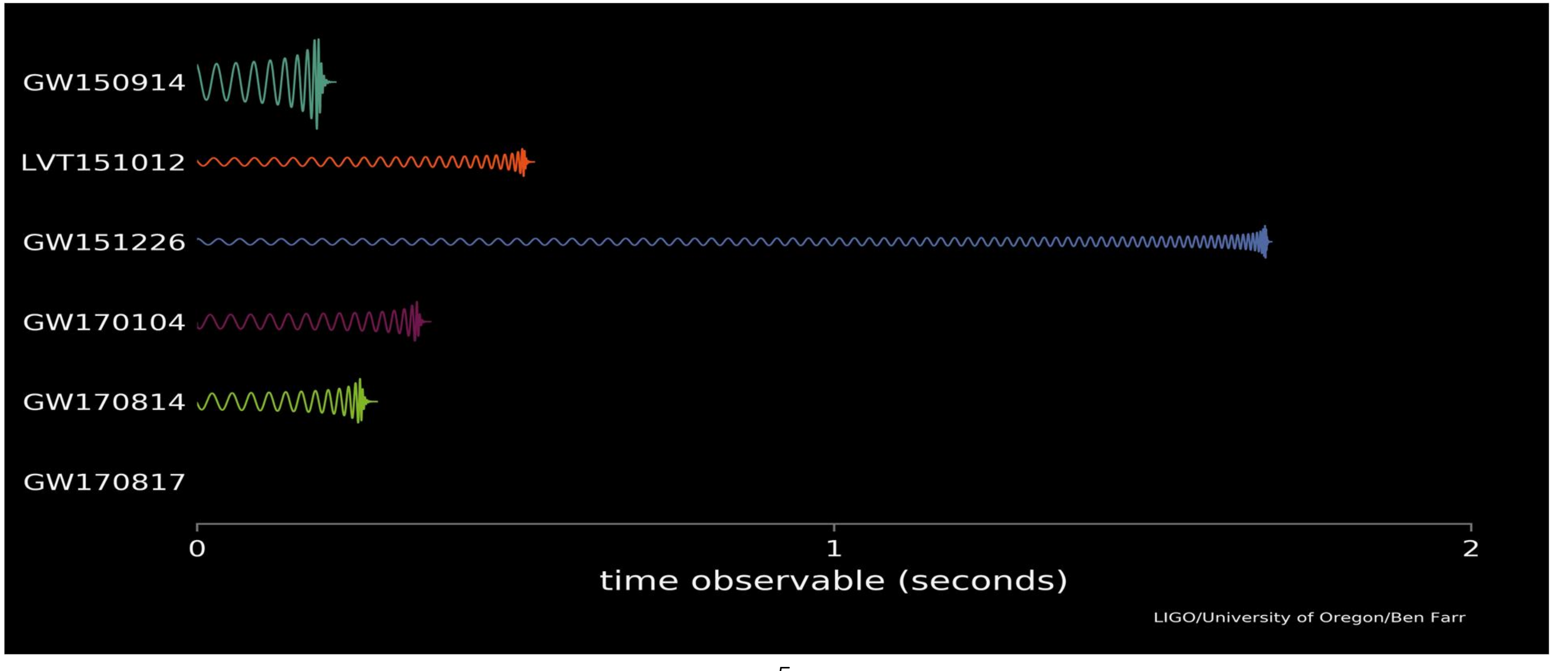

✓ Parameter estimations using signals observed:

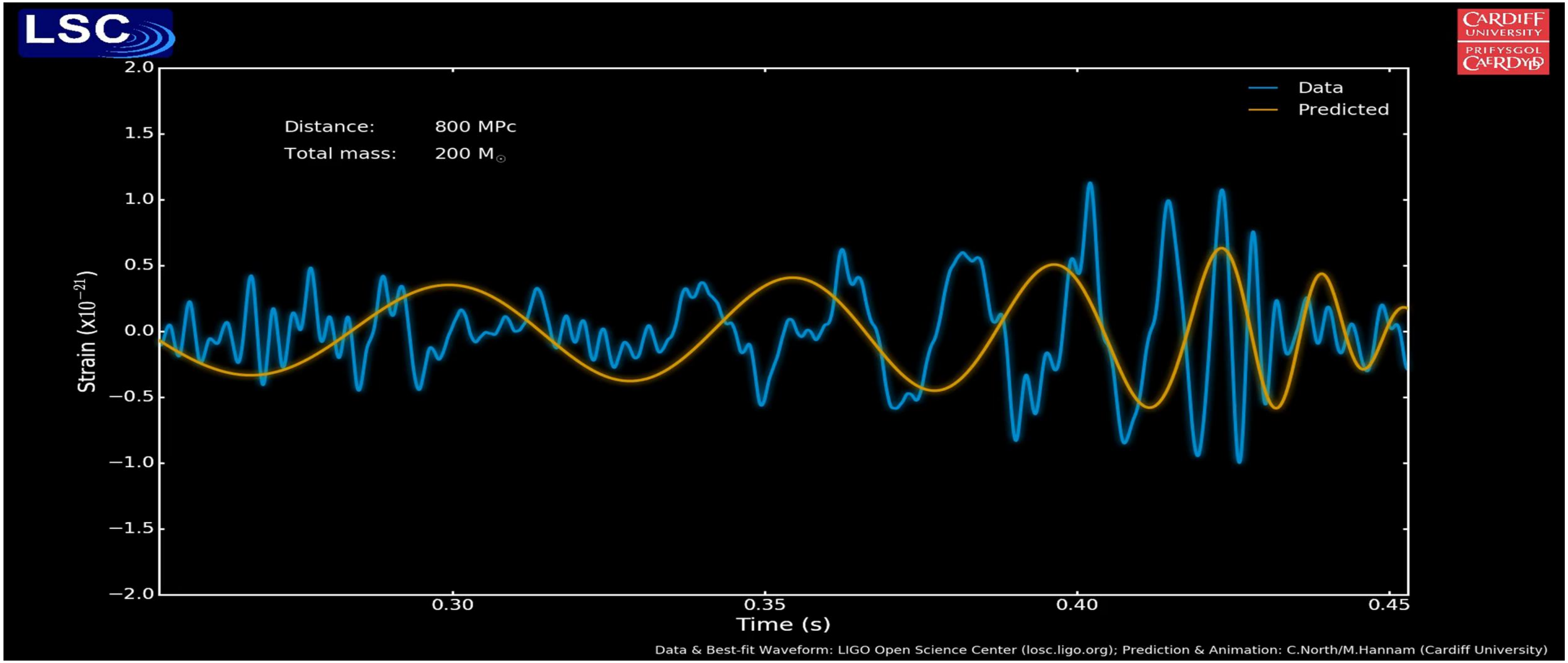

- Parameters for the GW sources obtained:

	GW150914	GW151226	GW170104	GW170608	GW170814	GW17081
Source	BBH	BBH	BBH	BBH	BBH	BNS
Signal-to-noise ratio	23.7	13.0	13	13	13.7	32.4
Primary mass ($M_\odot$)	$36.2^{+5.2}_{-3.8}$	$14.2^{+8.3}_{-3.7}$	$31.2^{+8.4}_{-6.0}$	12^{+7}_{-2}	$30.5^{+5.7}_{-3.0}$	1.36-1.60
Secondary mass ($M_\odot$)	$29.1^{+3.7}_{-4.4}$	$7.5^{+2.3}_{-2.3}$	$19.4^{+5.3}_{-5.9}$	7^{+2}_{-2}	$25.3^{+2.8}_{-4.2}$	1.17-1.36
Chirp mass ($M_\odot$)	$28.1^{+1.8}_{-1.5}$	$8.9^{+0.3}_{-0.3}$	$21.1^{+2.4}_{-2.7}$	$7.9^{+0.2}_{-0.2}$	$24.1^{+1.4}_{-1.1}$	$1.188^{+0.00}_{-0.00}$
Final mass ($M_\odot$)	$62.3^{+3.7}_{-3.1}$	$20.8^{+6.1}_{-1.7}$	$48.7^{+5.7}_{-4.6}$	$18^{+4.8}_{-0.9}$	$53.2^{+3.2}_{-2.5}$	
Final spin	$0.68^{+0.05}_{-0.06}$	$0.74^{+0.06}_{-0.06}$	$0.64^{+0.09}_{-0.20}$	$0.69^{+0.04}_{-0.05}$	$0.70^{+0.07}_{-0.05}$	
Luminocity distance (Mpc)	420^{+150}_{-180}	440^{+180}_{-190}	880^{+450}_{-390}	340^{+140}_{-140}	540^{+130}_{-210}	40^{+8}_{-14}
Tidal deformability $\tilde{\Lambda}$						≤ 800
Remark	O1, First direct detection	O1	O2	O2	O2 & Virgo	O2 & Virg

✓ GW170817: GWs from a BNS Inspiral

- First observation of a BNS inspiral on Aug. 17, 2017 at 12:41:04 UTC
- Duration: ~100 s, SNR: 32.4, FAR: ≤ One per 80,000 years

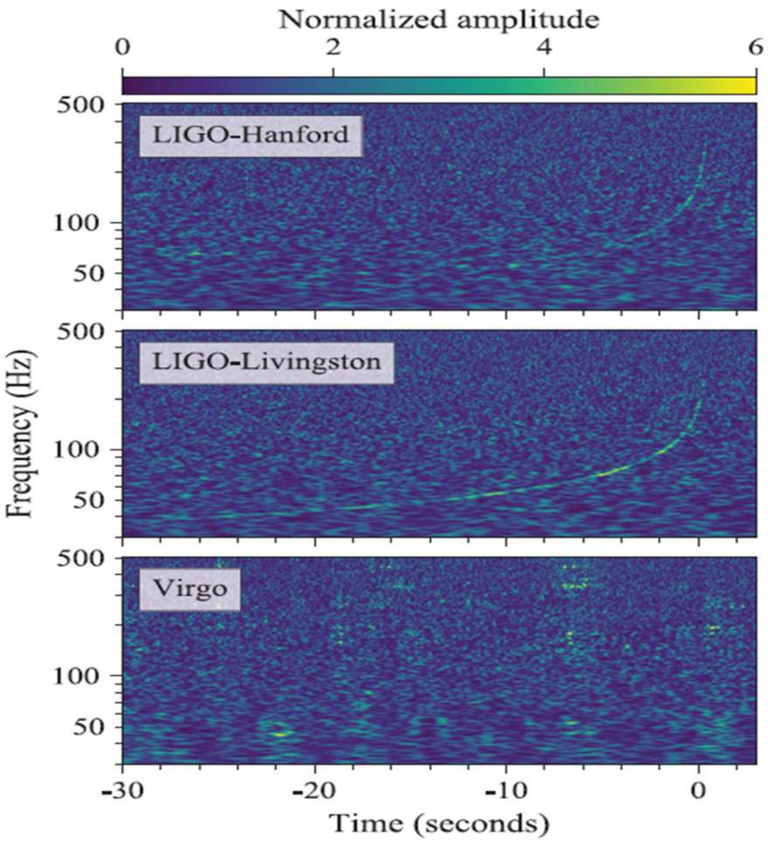

PRL **119**, 161101 (2017)

	Low-spin priors ($\|\chi\| \leq 0.05$)
Primary mass m_1	1.36–1.60 $M_\odot$
Secondary mass m_2	1.17–1.36 $M_\odot$
Chirp mass $\mathcal{M}$	$1.188^{+0.004}_{-0.002} M_\odot$
Mass ratio m_2/m_1	0.7–1.0
Total mass m_{tot}	$2.74^{+0.04}_{-0.01} M_\odot$
Radiated energy E_{rad}	$> 0.025 M_\odot c^2$
Luminosity distance D_L	40^{+8}_{-14} Mpc
Viewing angle Θ	$\leq 55°$
Using NGC 4993 location	$\leq 28°$
Combined dimensionless tidal deformability $\tilde{\Lambda}$	≤ 800
Dimensionless tidal deformability $\Lambda(1.4 M_\odot)$	≤ 800

- Radiation of EM waves was anticipated in.
- So, EM follow-up observation campaigns were launched immediately.

✓ Sky Localization and Optical Follow-up Observations:

$190\ deg^2$

$31\ deg^2$
(➔ $28\ deg^2$)

Near NGC 4993

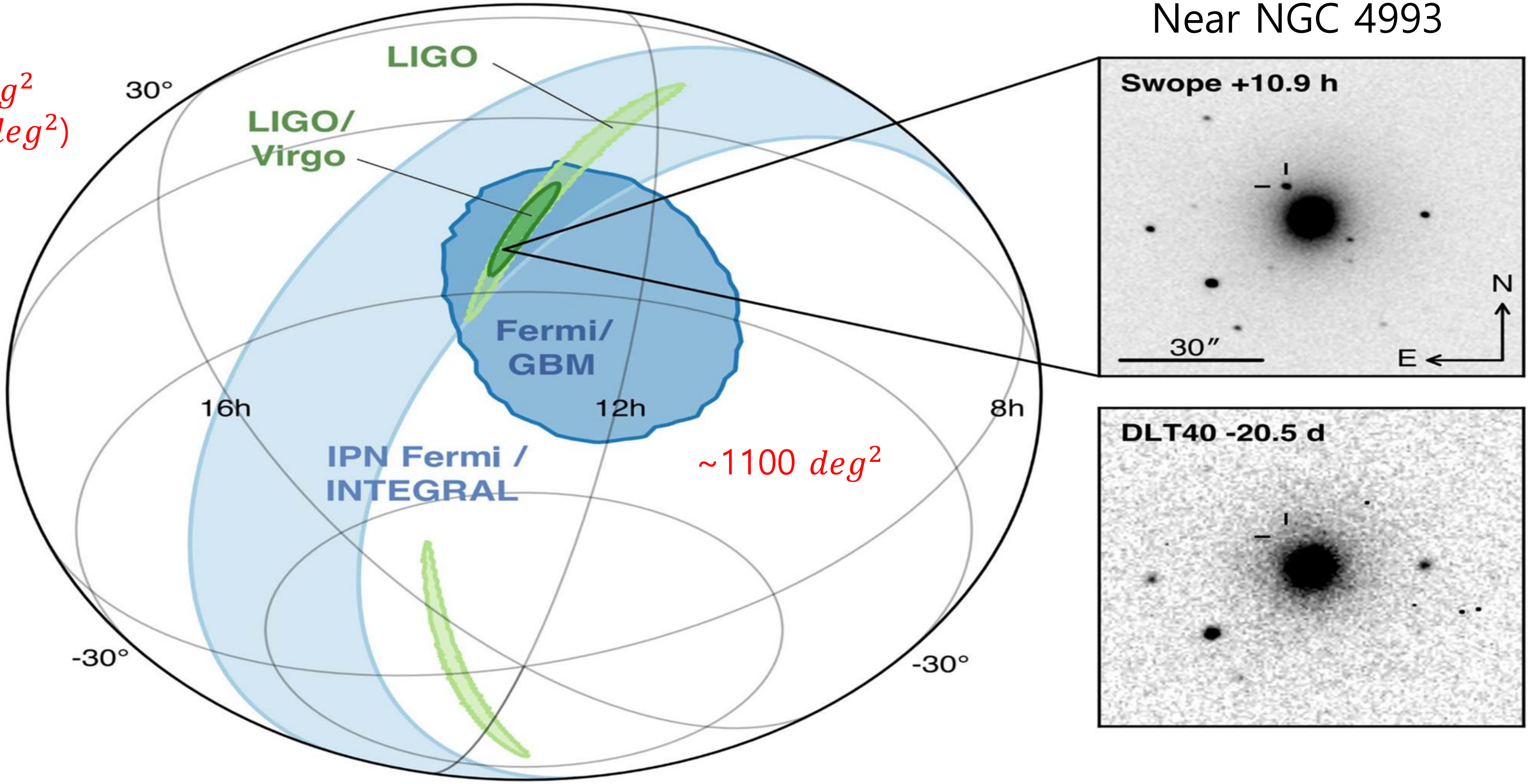

$\sim 1100\ deg^2$

Centered around $(12^h57^m, -17^\circ 51')$

ApJL ('17)

✓ Multi-Messenger Astronomy:

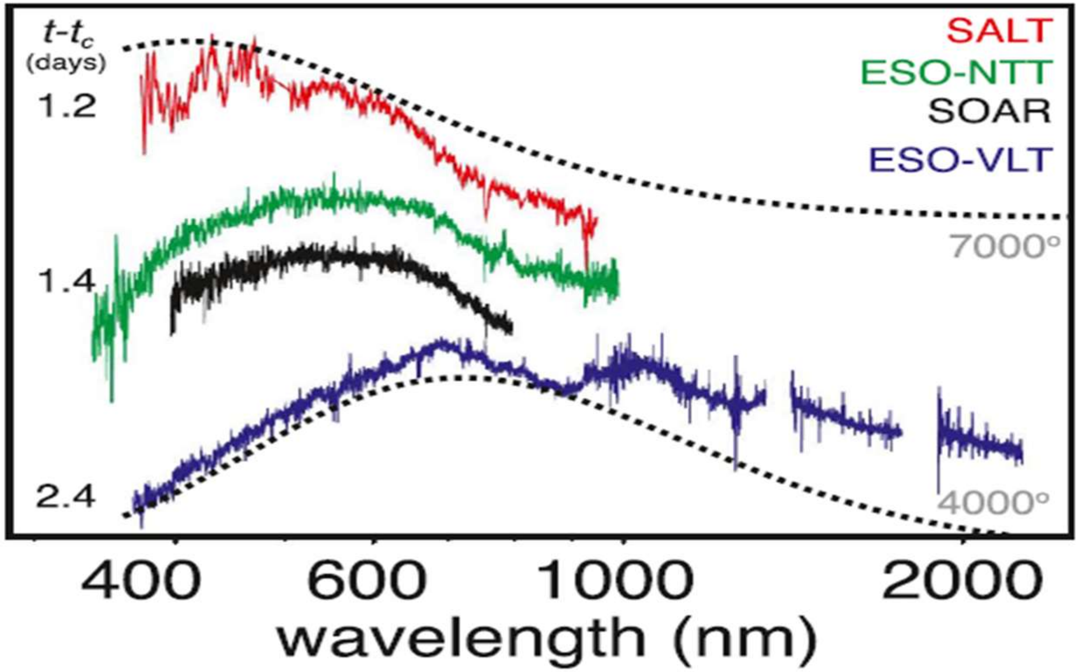

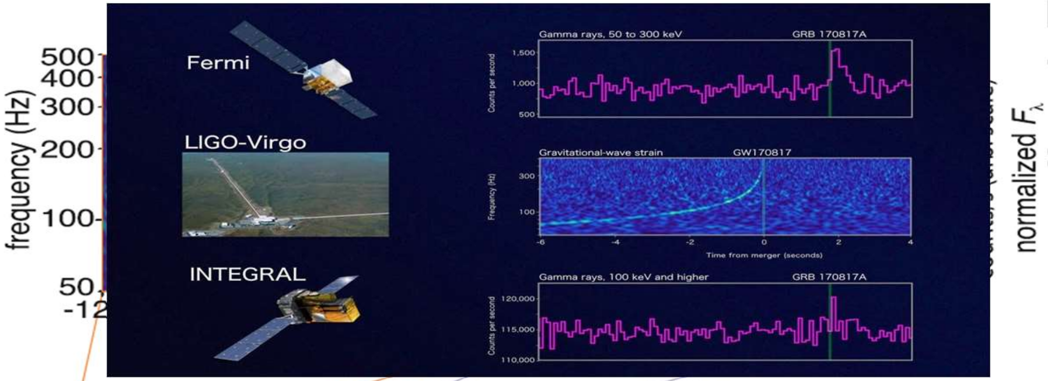

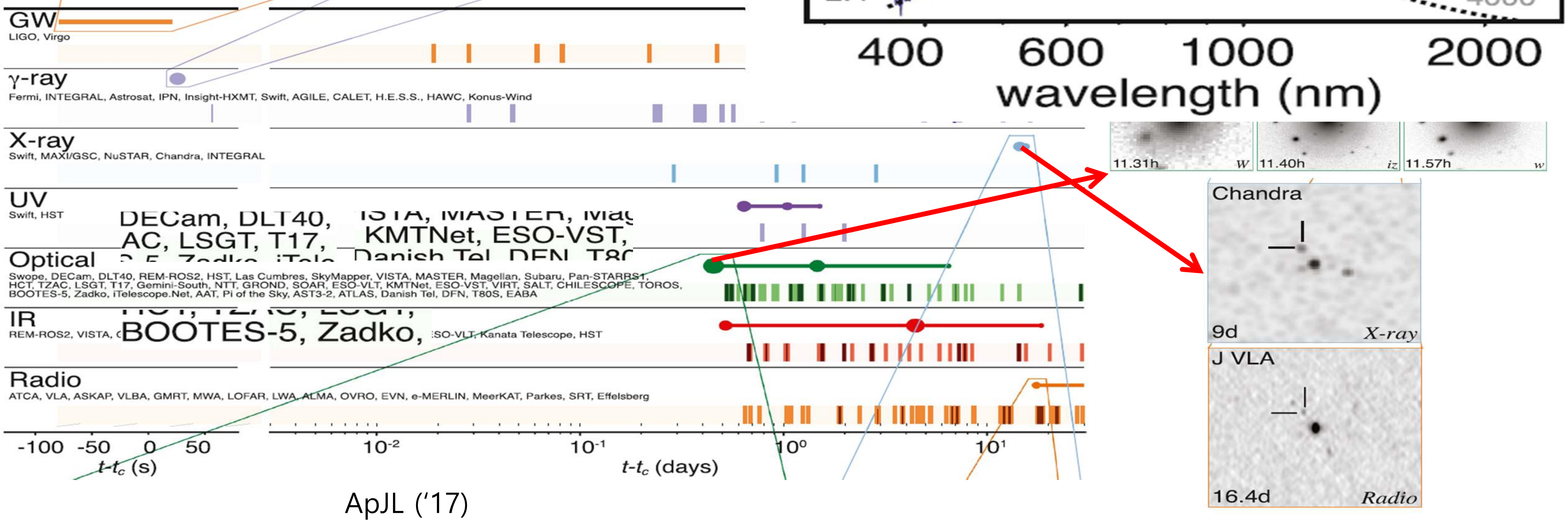

ApJL ('17)

✓ First secure identification of the factory of gold, platinum, uranium etc.

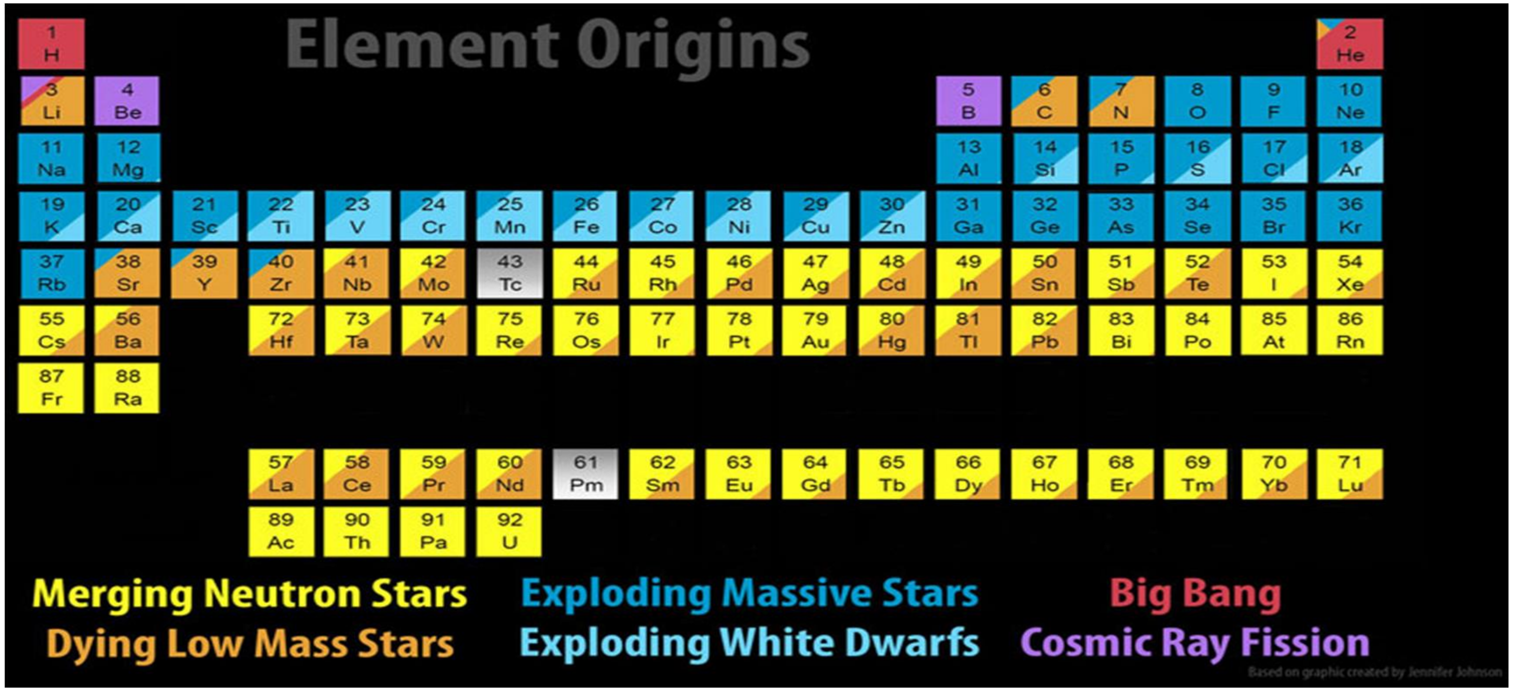

- Efficient neutron capture (r-process) leads to creation of these elements
- **200 earth mass gold**, 500 earth mass platinum

Slide credit: M. Im ('17)

✓ Optical Follow-up Observations in Korea:

- Lee Sang Gak Telescope (LSGT)
- Observed ~21 hrs after GW170817
- 0.43m at Siding Spring in Australia
- Seoul Nat'l U.

- Korea Microlensing Telescope Network (KMTNet)
- Observed ~28 hrs after GW170817
- 1.6m at S. Africa-Chille-Australia during Aug. 18~Sept. 07, 2017
- KASI/SNU

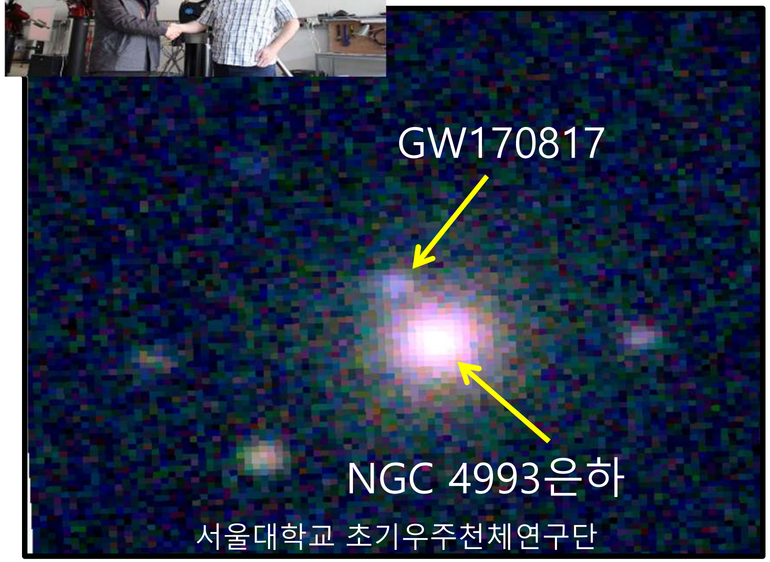

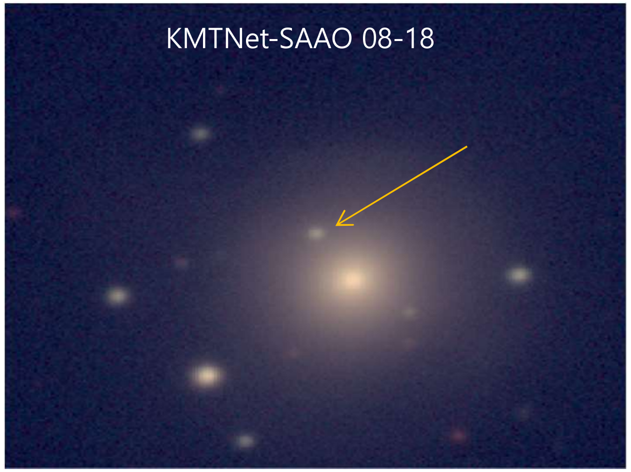

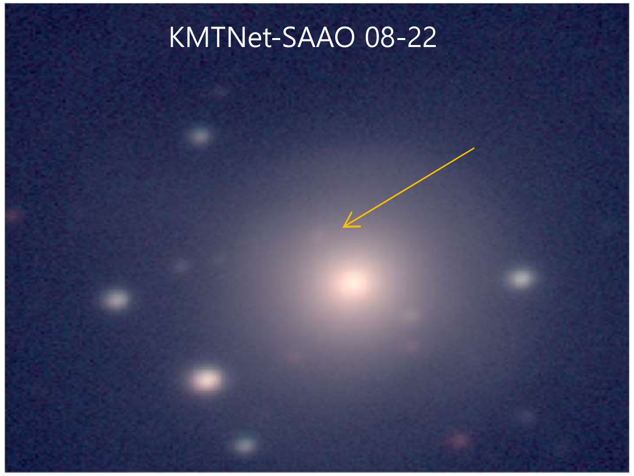

✓ Perspectives

- Evolution of the LIGO sensitivity
- O1: 2015/09/12~2016/01/12
- O2: 2016/11/30~2017/08/25
- O3: Early in 2019 with 2~4 better sensitivity ➔ 3~25 events per month!

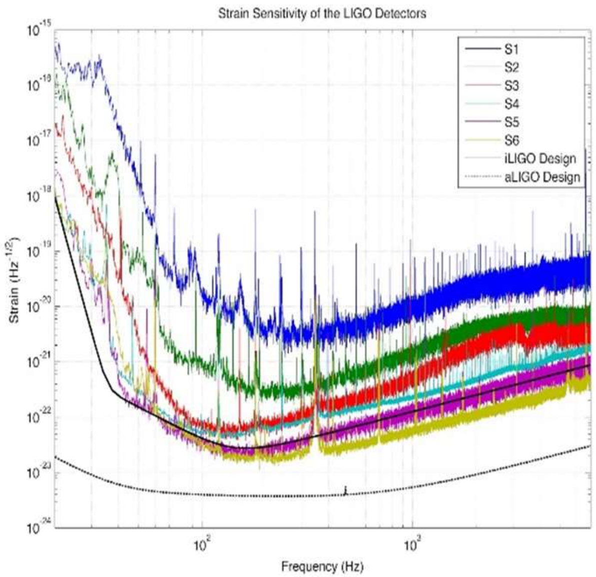

S1(2002)~S6(2010)

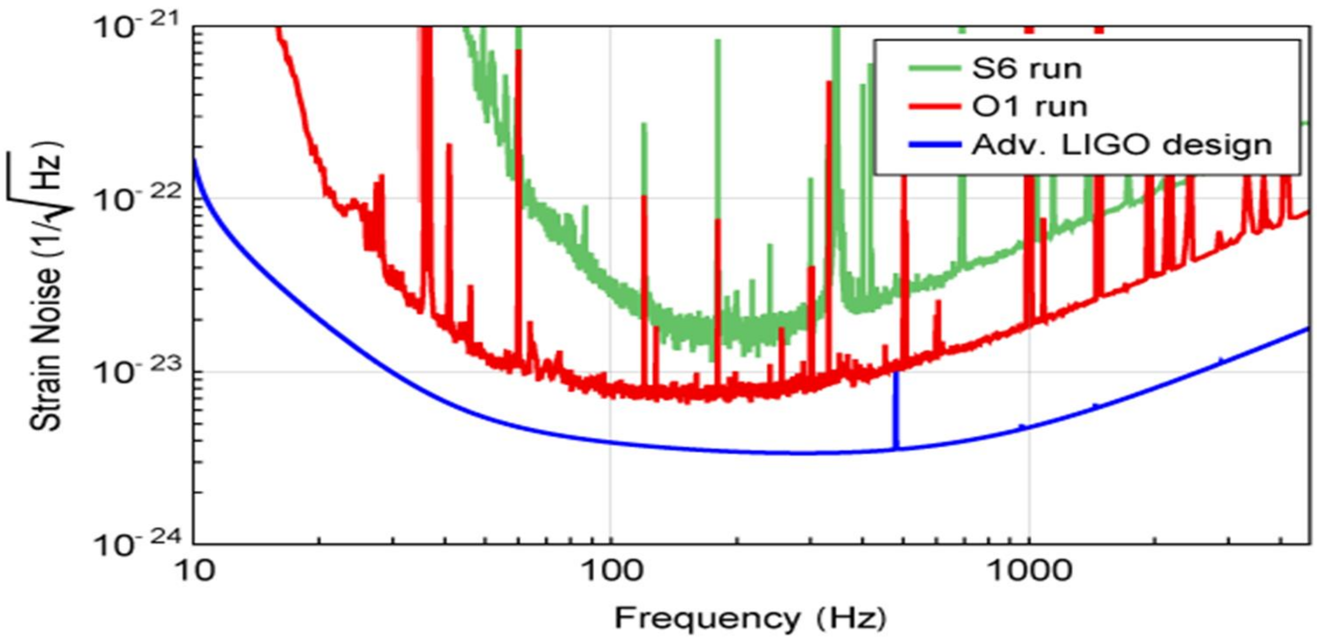

https://www.advancedligo.mit.edu/

Network of GW observatories

Laser Interferometer for Gravitational-wave Observation

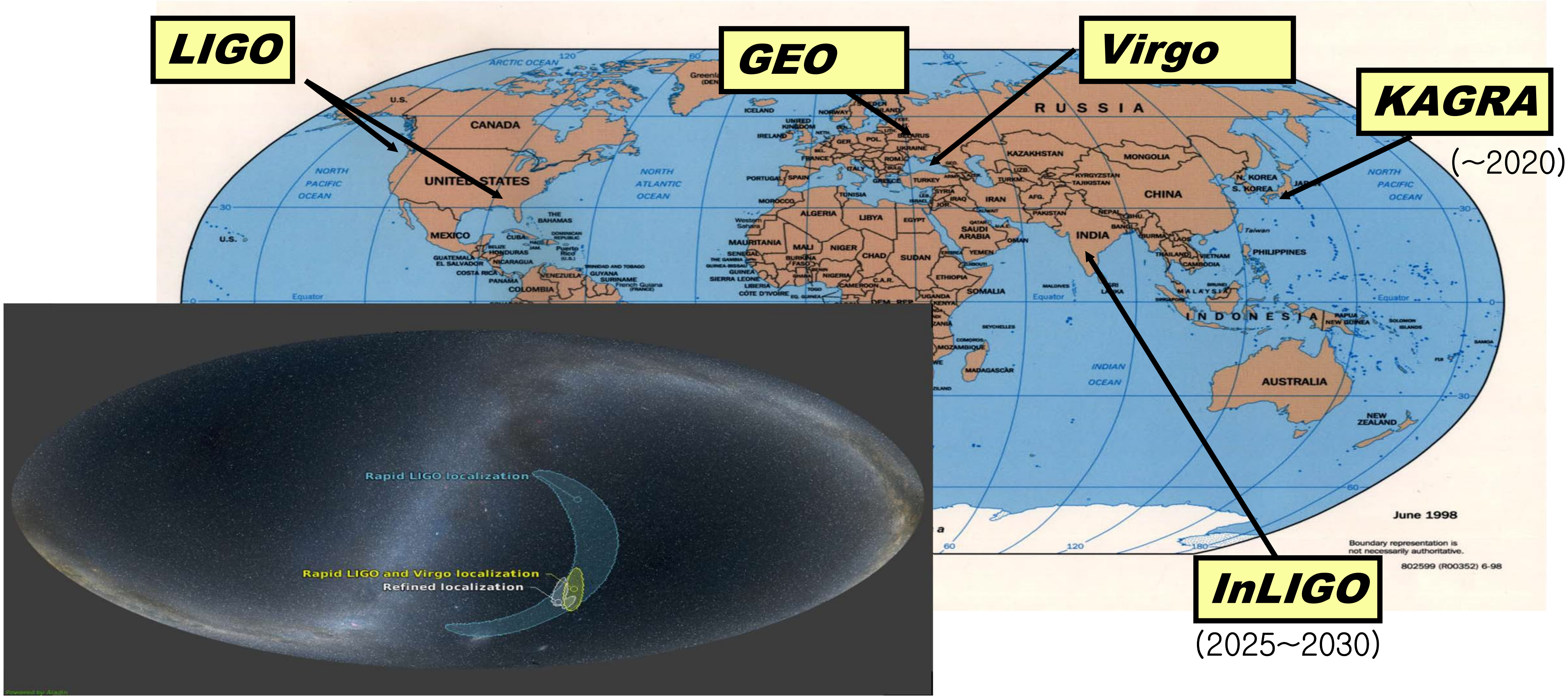

Better sky localization: ~10 times (GW170814)

Cited in part from H.J. Paik's talk

Making advanced LIGO better: A+

- Squeezing and coating required R&D required to increase the sensitivity beyond aLIGO
- Squeezing could be ready before aLIGO

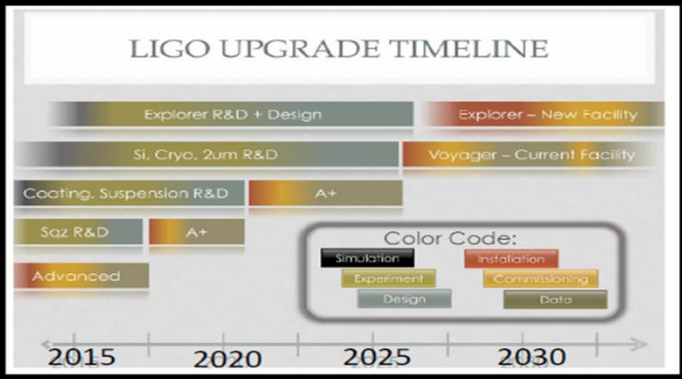

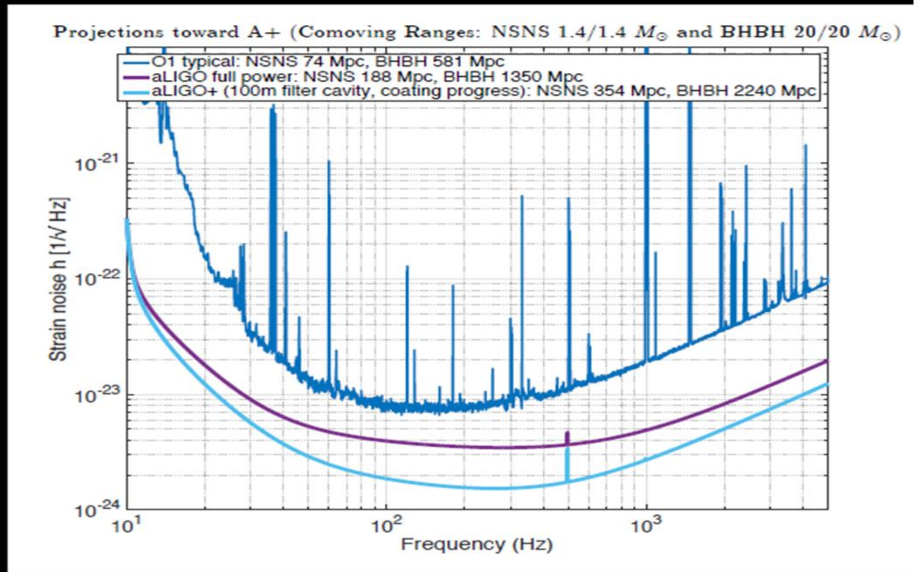

J. Miller , G1601807

Slide credit: S. Vitale

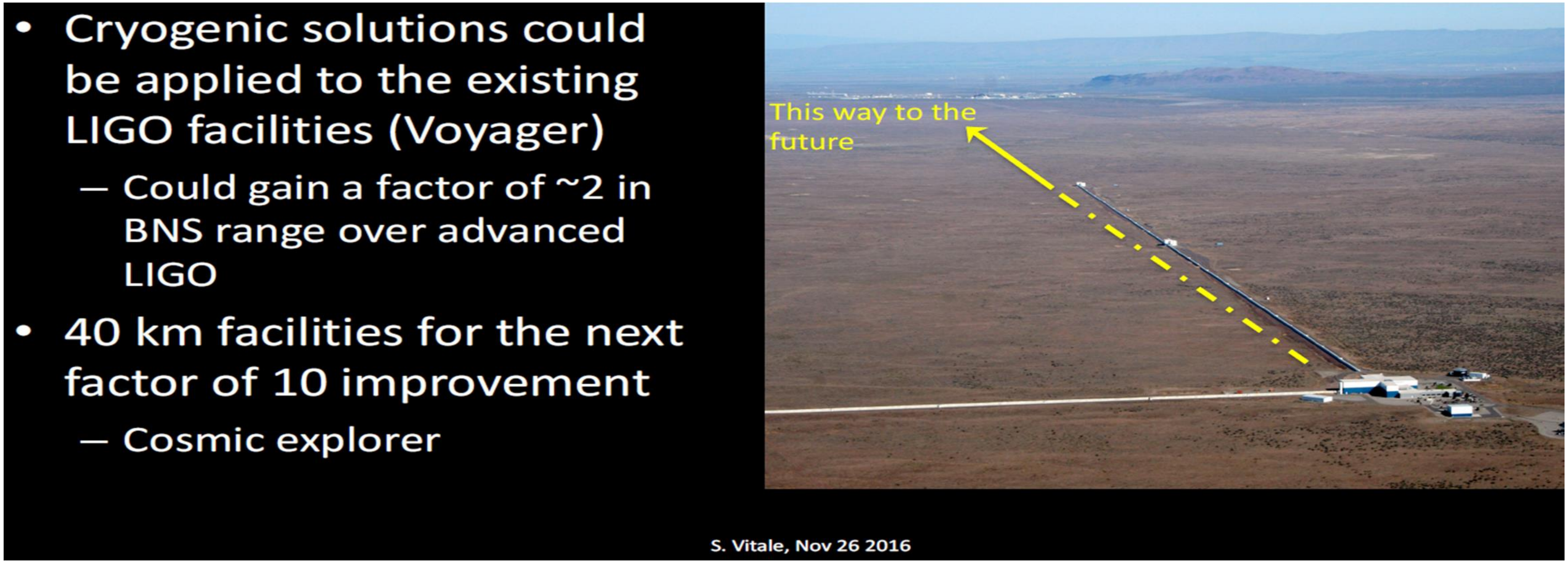

Slide credit: S. Vitale

Future Gravitational Wave Detectors

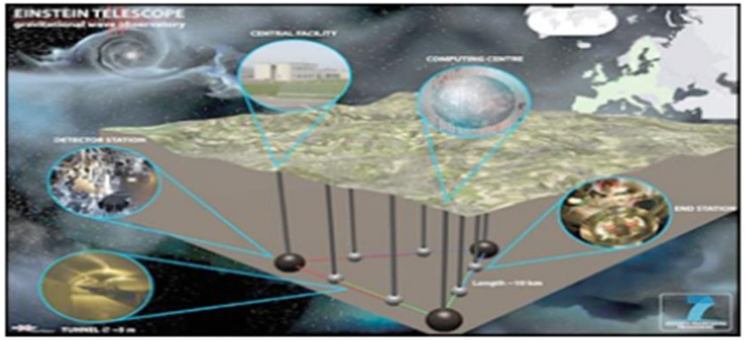

Einstein Telescope (ESA)

2030? (designing stage)

eLISA

(NGO)

2020?

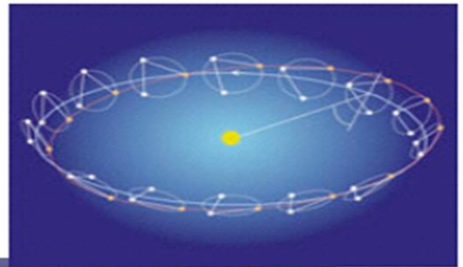

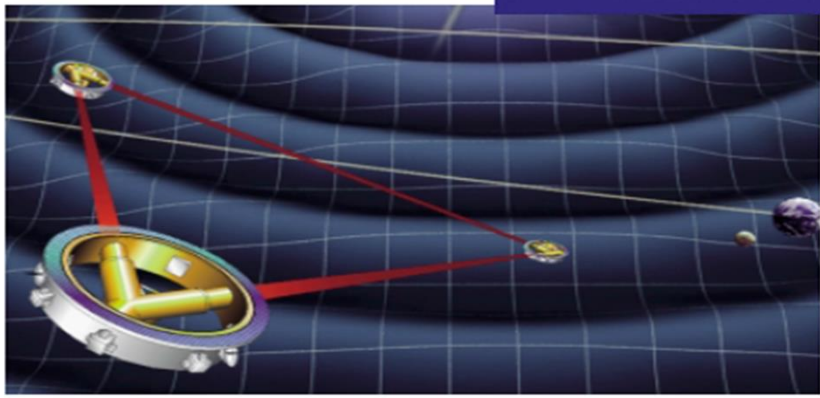

- **Timelines: A+ (~2022), AdV+, Voyager (~2025), Einstein Telescope (~2023), Cosmic Explorer (~2027), DECIGO (~2027), TianQin (?), …**

Comparisons:

EM waves

- Theory: Maxwell (1864)
- Detection: H. Hertz (1886)

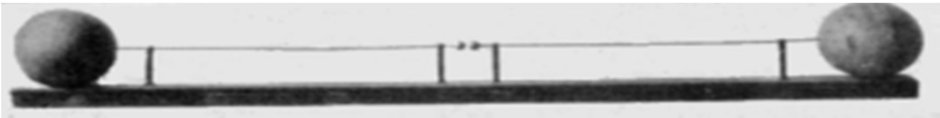

GW

- Theory: Einstein (1916)
- Detection: LIGO(2015)

Weber (1960)

LIGO

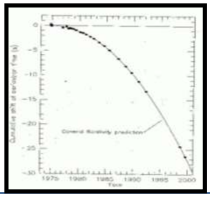

Hulse & Taylor (1975)

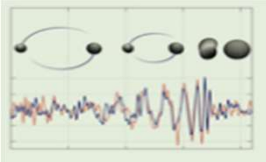

- Applications:

(~1990)

??

(~2500 (?))

✓ How big is the gap?

- Use GWs for telecommunications for example:
  - Absorption distance for E ➔ E/2 in water: $\sim 10^{29}$ km
    ~0.1 billion times larger than the size of our observed universe!
  - Current capability of receiving: $10^{-21} \sim 10^{-23}$
  - Strength of a GW generation surround: $h_{GW} \sim 10^{-40}$
  - Currently, the gap is $\sim 10^{20}$!!
- For LIGO, it took ~13 years to have an improvement of $\sim 10^{3}$.
- Maybe the solution would be "Quantum Effect": $\sim G/\hbar$

- ✓ “Echoes after the merger signal” by Abedi et al (‘17)
  ➔ Supports “Fire-wall”

- ✓ Check by Alex Nielsen

- Searched for by non-LIGO team using templates: 1612.00266
- Original claimed significance was **2.9 sigma (p-value 0.011)**

Our combined significance estimate for these signals is ~1.3σ (p-value 0.104).

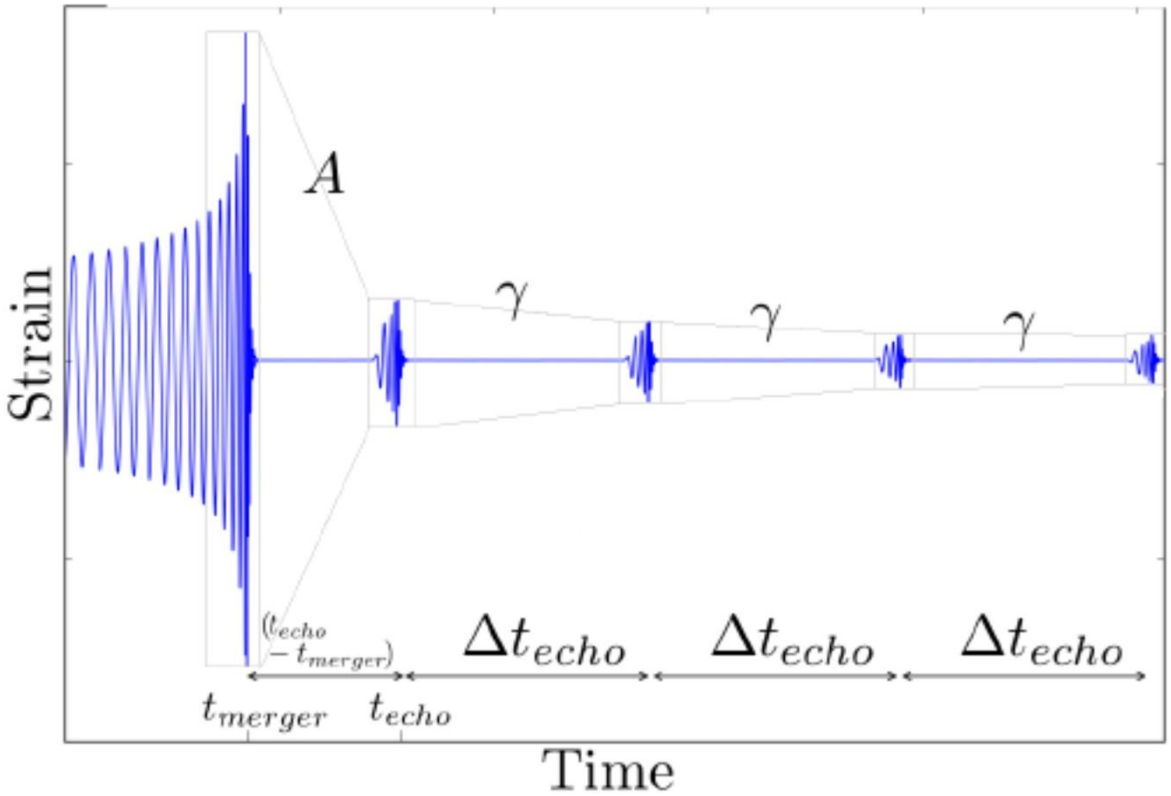

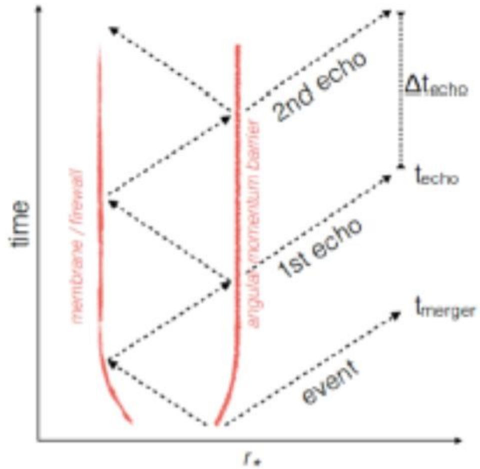

✓ Gravitational wave spectrum, detectors and sources:

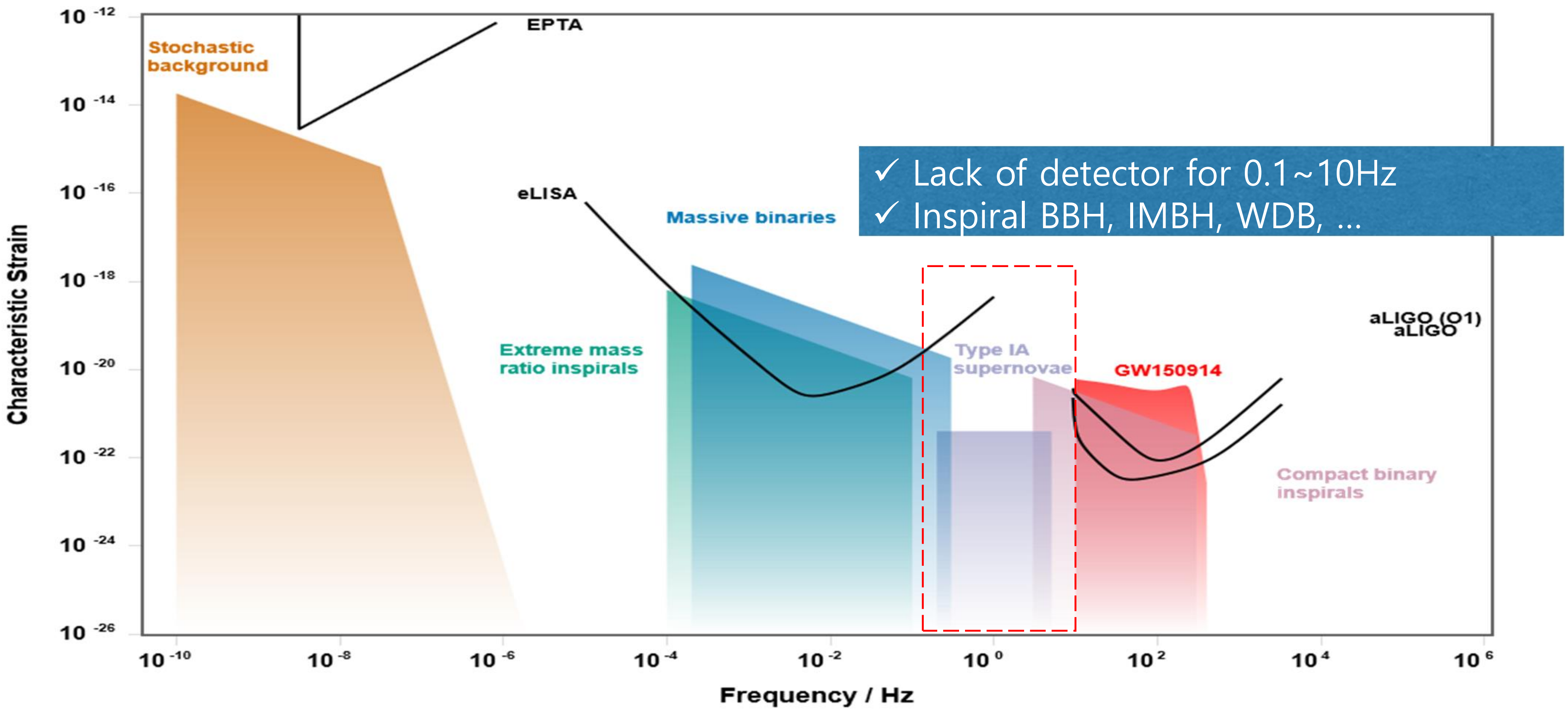

http://rhcole.com/apps/GWplotter/
by Moore, Cole & Berry

II. Introduction to SOGRO

✓ Obstacles in low frequencies, *e.g.,* 0.1~10Hz:

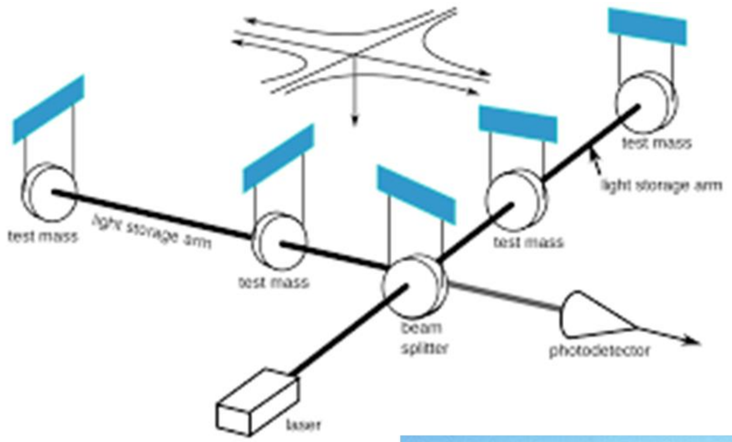

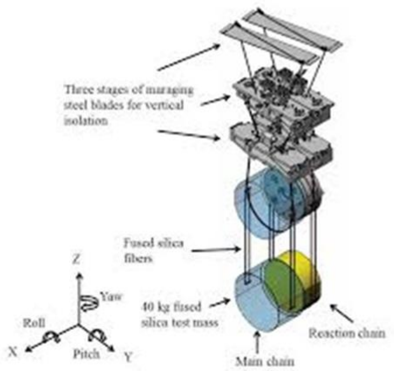

Mainly due to

✓ Ground motions ➔ **Seismic noise**

✓ Density fluctuations in Earth and atmosphere around the mirrors

➔ **Varying gravity**

➔ **Newtonian gravity noise**

✓ **Characteristic frequencies:**

"Low Frequencies"

✓ DECIGO (Deci-hertz interferometer Gravitational-wave Observatory)

- Same interferometer detector, but put it into space to avoid such noises!
- ~2027

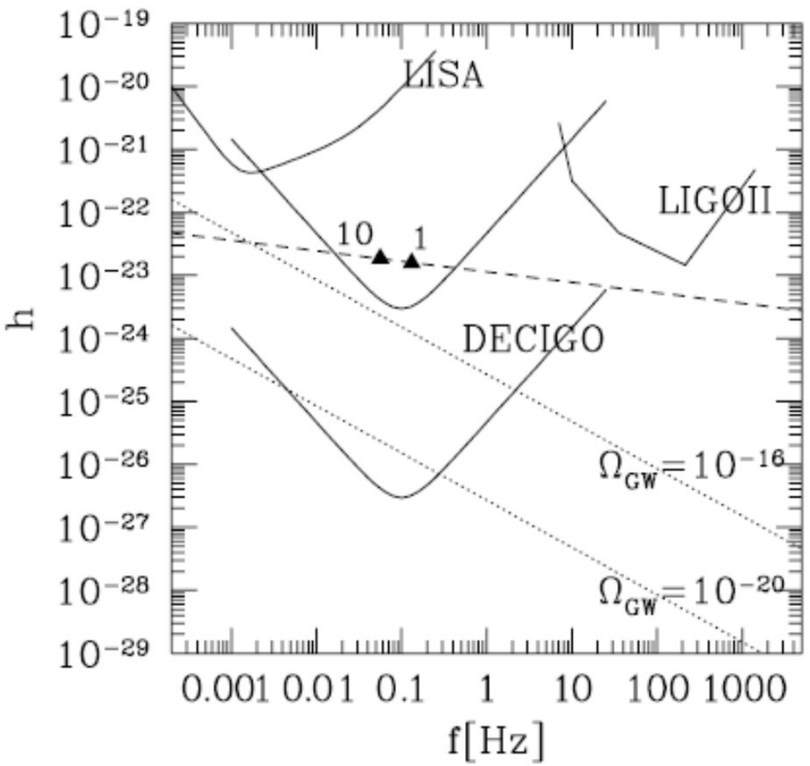

Seto, Kawamura & Nakamura (2001)

Roadmap (Slide credit: M. Ando 2012)

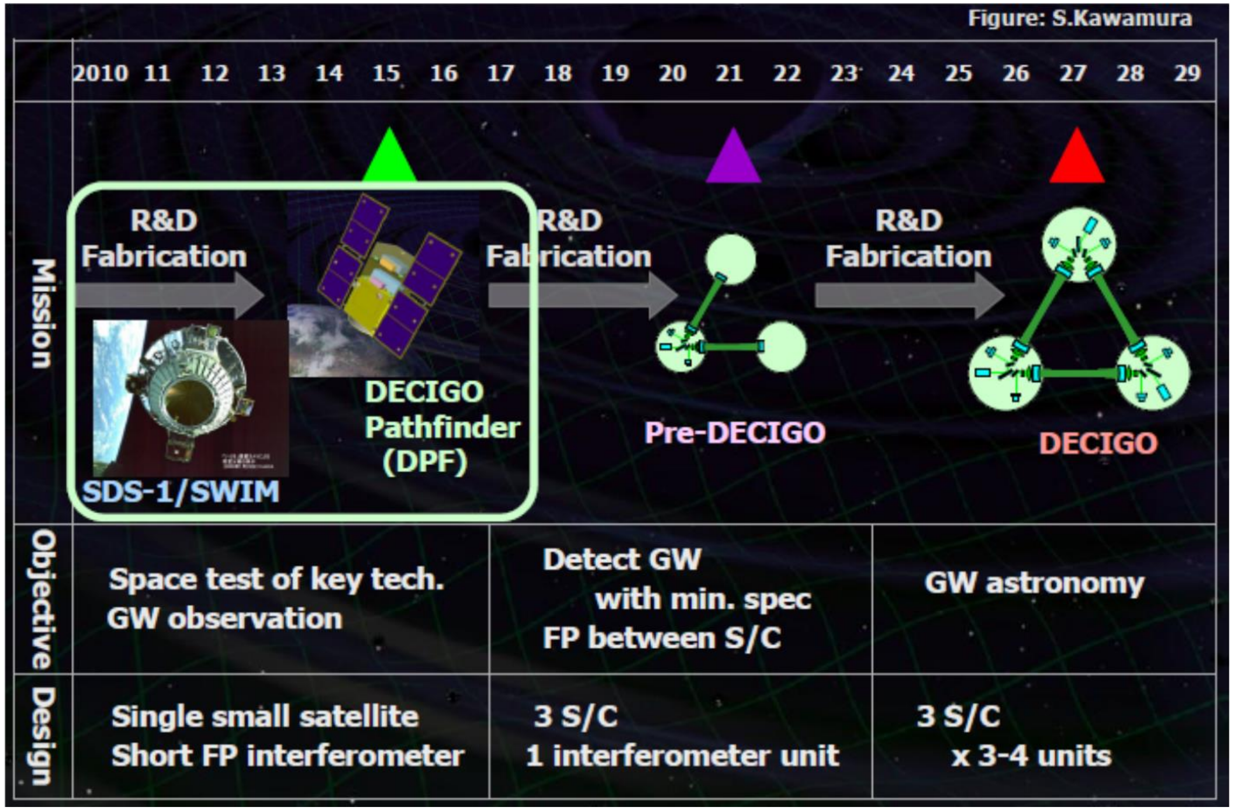

✓ What about terrestrial antenna at low frequencies?

- Wagoner, Will & Paik: 1979
- Superconducting Gravity Gradiometer (SGG):

Ho Jung Paik

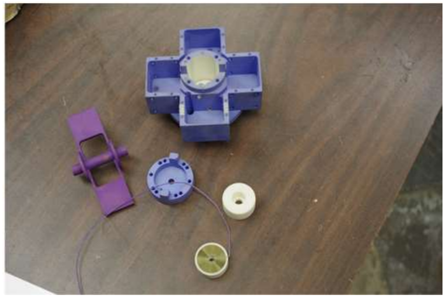

(Picture credit: H-M. Lee)

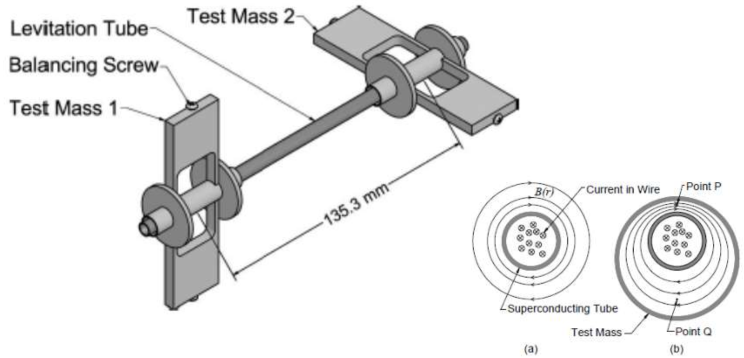

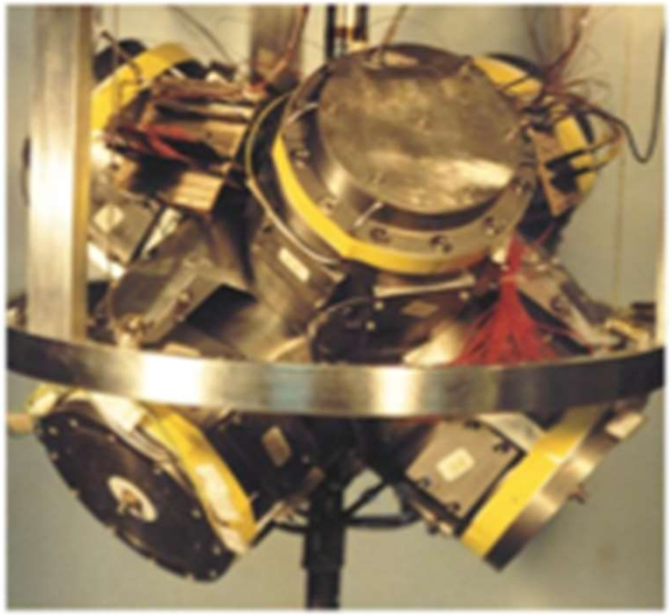

Moody, Paik, & Caravan (2002)

✓ Measure the **relative motion of test masses**

✓ Magnetic levitation, SQUID sensor

✓ Test mass: 25kg, Size: 30cm

✓ Sensitivity: $\sim 2 \times 10^{-11} s^{-2} Hz^{-1/2}$

✓ Developed for over 30 years at U. of Maryland

1. Design and Principle

❖ Chan & Paik, PRD (1987):

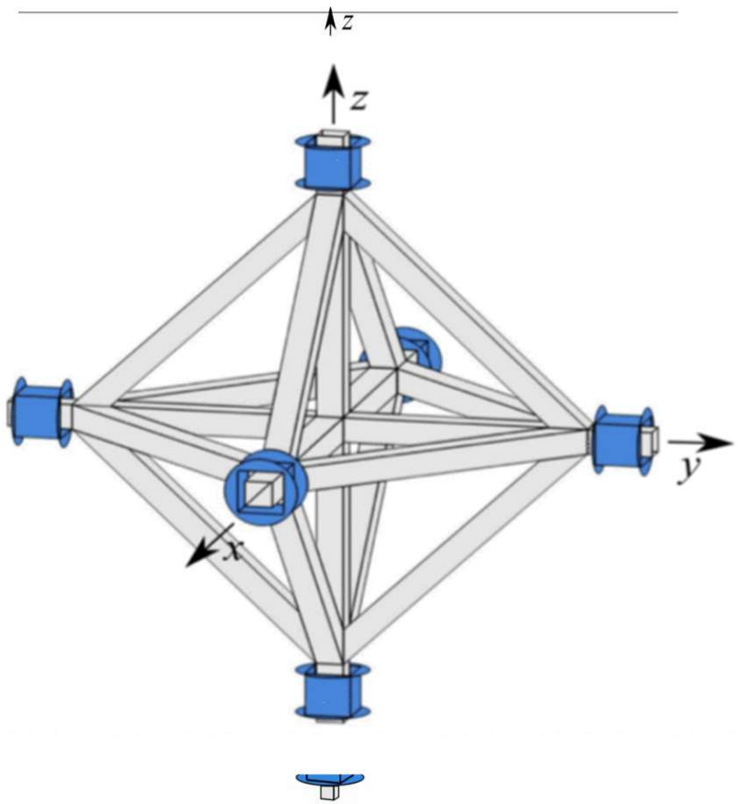

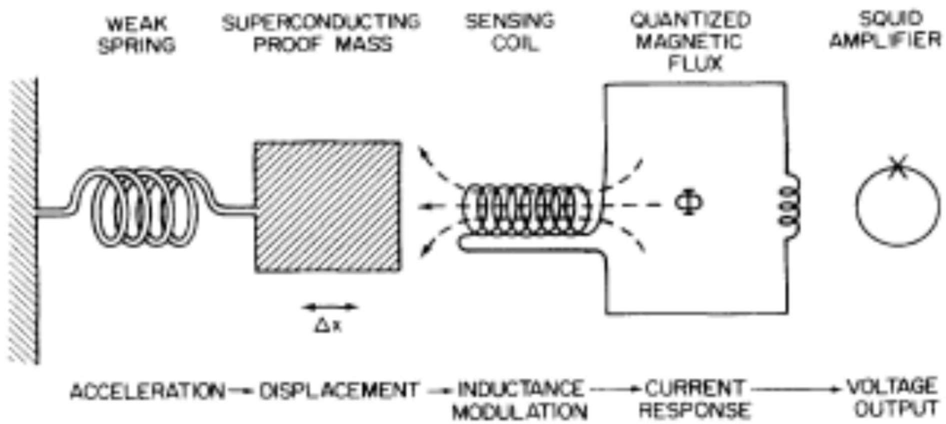

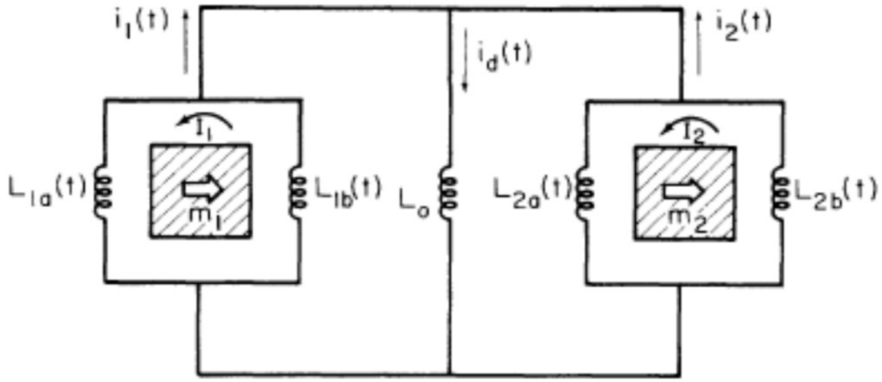

➔ **Only relative motions matter!!**

- Combining 6 test masses, a tensor GW detector is formed;

$$h_{ii}(t) = \frac{2}{L}\left[x_{+ii}(t) - x_{-ii}(t)\right]$$

$$h_{ij}(t) = \frac{1}{L}\left\{\left[x_{+ij}(t) - x_{-ij}(t)\right] - \left[x_{-ji}(t) - x_{+ji}(t)\right]\right\}, i \neq j$$

- Thus, the source direction $(\theta, \emptyset)$ and GW polarizations can be determined by a single antenna. ➔ "Spherical Antenna"

- **SOGRO**: **S**uperconducting **O**mni-directional **G**ravitational **R**adiation **O**bservatory

Table 7. Responses of off-diagonal, diagonal and total sum of tensor components.

components	F_+	$F_\times$	F_{tot}
off-diagonal	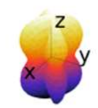		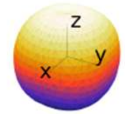
diagonal	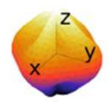	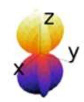	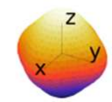
total	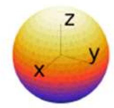	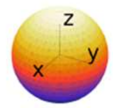	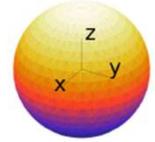

✓ However, there are noises!

✓ Main noise sources:

- Antenna noise: Test mass
- Amplifier noise: SQUID

$$S_h(f) = \frac{32}{ML^2\omega^4}\left\{\frac{k_B T\omega_D}{Q_D} + \frac{\left|\omega^2 - \omega_D^2\right|}{2\omega_p}\left(1 + \frac{1}{\beta^2}\right)^{1/2} k_B T_N\right\}, \; k_B T_N = n\eta\omega_p$$

- Platform thermal noise

$$S_{\xi,\omega_0}(f) = \frac{16}{m_{\text{eff}} L^2 \omega_0^2 Q_{\text{pl}} \omega} \frac{4k_B T_{\text{pl}}}{(1-\omega^2/\omega_0^2)^2 + 1/Q_{\text{pl}}^2}. \qquad S_\xi(f) = \sum_i S_{\xi,\omega_{0i}}(f)$$

- Newtonian noise

✓ **Noise budget:**

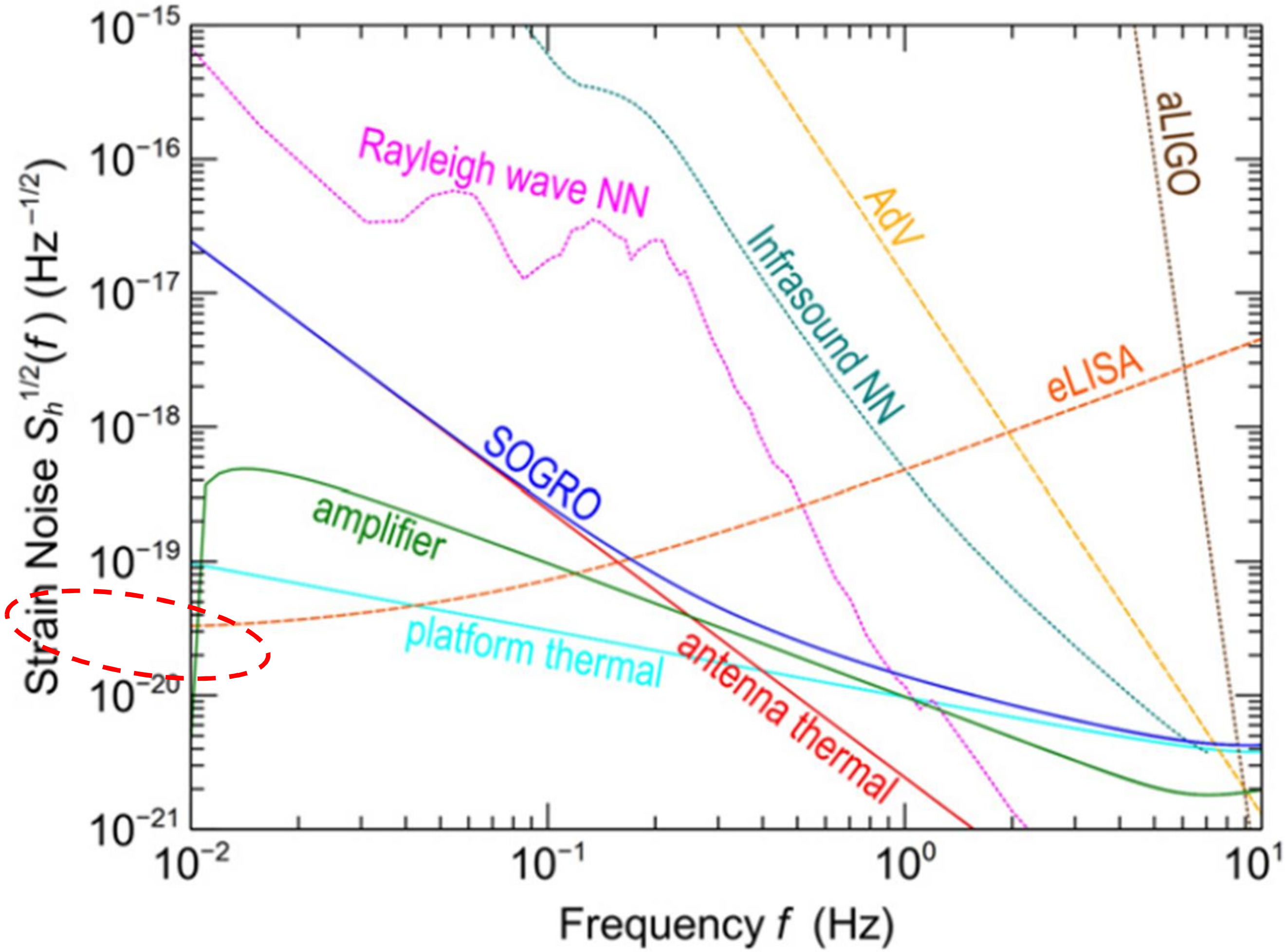

✓ Pre-stressed modal analyses of the platform structure: FEM using ANSYS

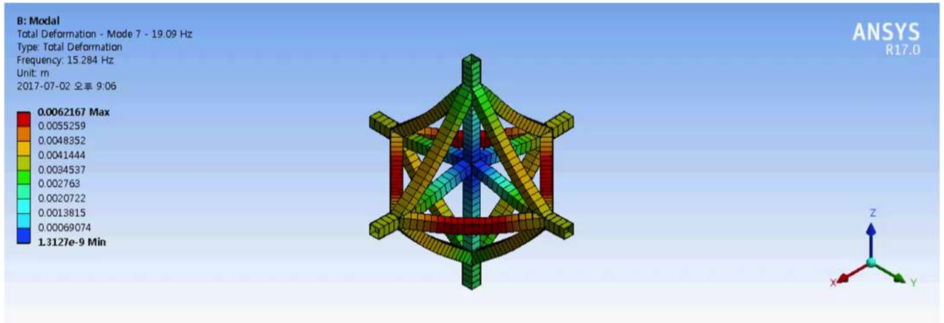

Mode 6 @ 15.284Hz : Common mode

Mode 7 @ 19.09Hz : Scissor mode

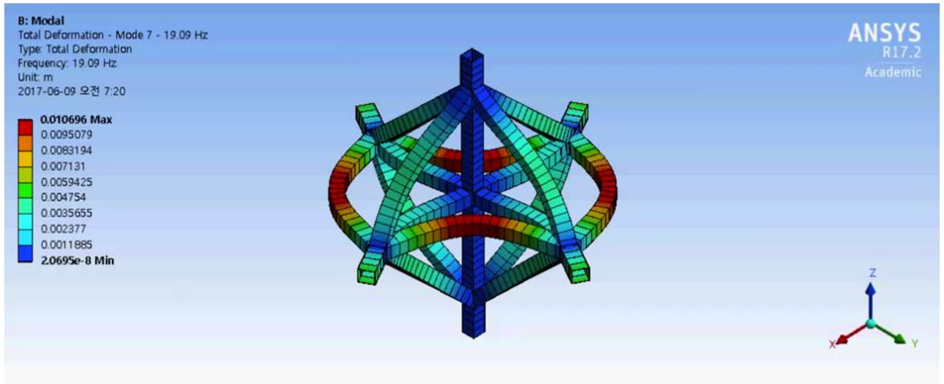

Mode 27 @ 29.878Hz : Diagonal mode

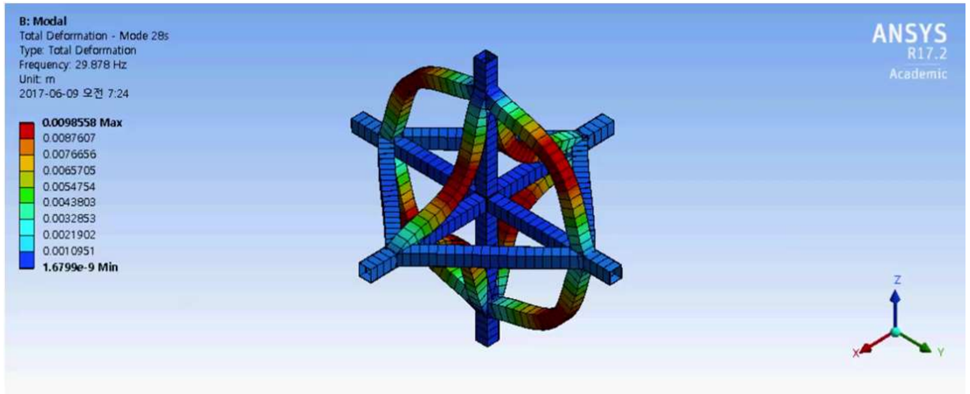

✓ Platform strain noise:

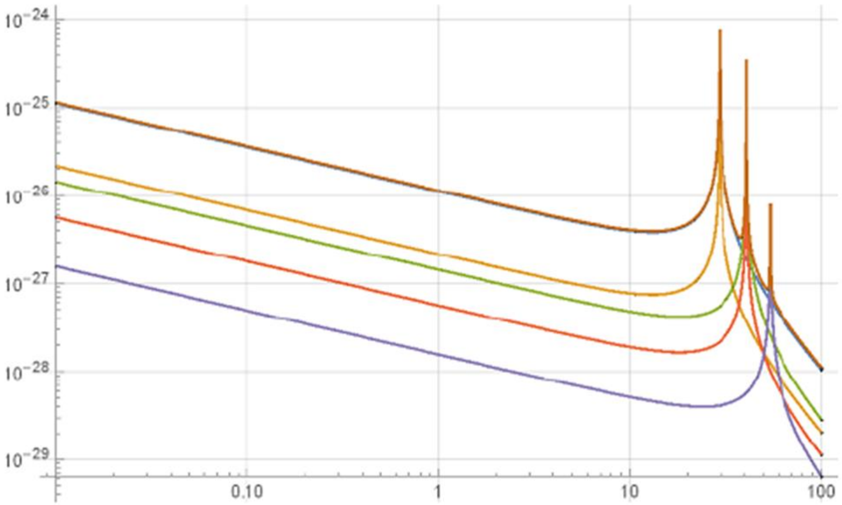

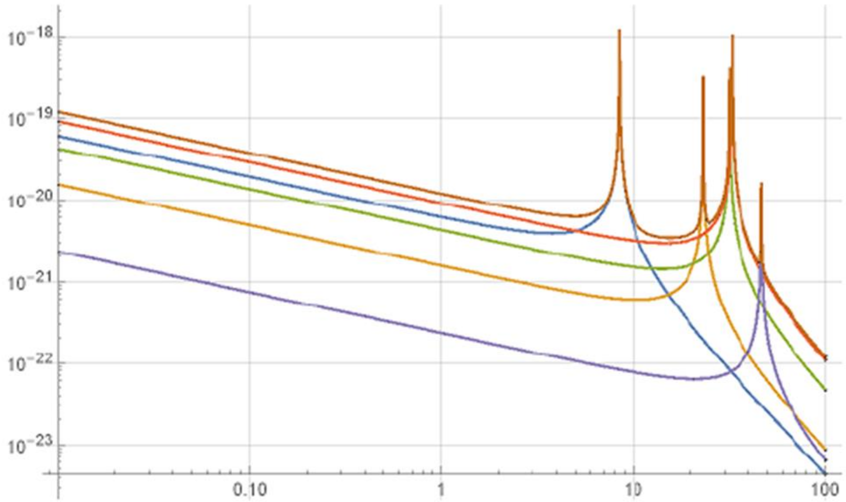

aSOGRO

XX-Modes

XY-Modes

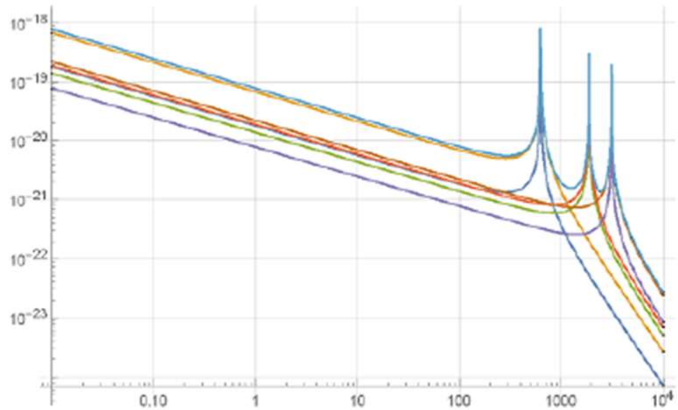

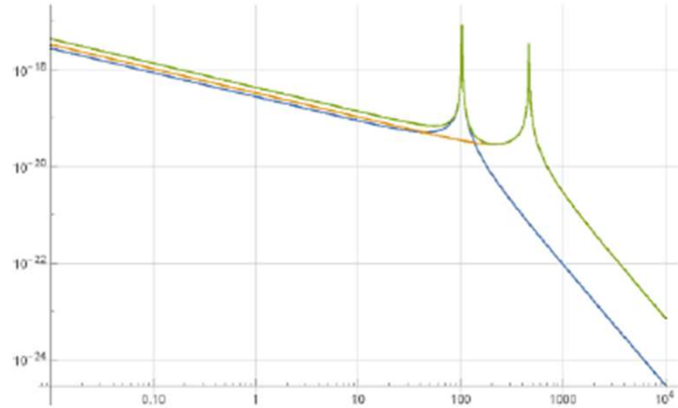

pSOGRO

✓ Newtonian noise mitigation: Go to underground first and use seismometers, microphones, Wiener Filter and SOGRO measurements (Harms *et al* '16)

In the GW coordinate system,

$$h'(\omega) = \begin{pmatrix} h_+(\omega) + h'_{N11}(\omega) & h_\times(\omega) + h'_{N12}(\omega) & h'_{N13}(\omega) \\ h_\times(\omega) + h'_{N12}(\omega) & -h_+(\omega) + h'_{N22}(\omega) & h'_{N23}(\omega) \\ h'_{N13}(\omega) & h'_{N23}(\omega) & h'_{N33}(\omega) \end{pmatrix}, \text{ where}$$

$$h'_{N11}(\omega) = \sum_i \left[a(\omega)\xi_i(\omega) + b(\omega,\vartheta_i)\delta\rho_i(\omega)\right][\cos(\psi_i - \phi)\cos\theta + i\sin\theta]^2$$

$$h'_{N22}(\omega) = \sum_i \left[a(\omega)\xi_i(\omega) + b(\omega,\vartheta_i)\delta\rho_i(\omega)\right]\sin^2(\psi_i - \phi)$$

$$h'_{N33}(\omega) = \sum_i \left[a(\omega)\xi_i(\omega) + b(\omega,\vartheta_i)\delta\rho_i(\omega)\right][\cos(\psi_i - \phi)\sin\theta - i\cos\theta]^2$$

$$h'_{N12}(\omega) = \sum_i \left[a(\omega)\xi_i(\omega) + b(\omega,\vartheta_i)\delta\rho_i(\omega)\right]\sin(\psi_i - \phi)[\cos(\psi_i - \phi)\cos\theta + i\sin\theta]$$

$$h'_{N23}(\omega) = \sum_i \left[a(\omega)\xi_i(\omega) + b(\omega,\vartheta_i)\delta\rho_i(\omega)\right]\sin(\psi_i - \phi)[\cos(\psi_i - \phi)\sin\theta - i\cos\theta]$$

$$h'_{N13}(\omega) = \sum_i \left[a(\omega)\xi_i(\omega) + b(\omega,\vartheta_i)\rho_i(\omega)\right][\cos(\psi_i - \phi)\cos\theta + i\sin\theta][\cos(\psi_i - \phi)\sin\theta - i\cos\theta]$$

$$h_+ = h'_{11} - 2\cot(\theta)h'_{13} + \cot^2(\theta)h'_{33} + \csc^2(\theta)2\pi\gamma G\rho_0 \frac{k}{\omega^2}\sum_i \xi_i(\omega) + \csc^2(\theta)\frac{4\pi}{\omega^2}\frac{G\rho_0}{\gamma p_0}\sum_i \delta p_i(\omega)\sin^2(\beta_i)$$

✓ Design parameters:

Parameter	pSOGRO	aSOGRO	Method employed
Each test mass M	100 kg	5 ton	Multiple-layer Nb shell
Arm-length L	2 m	50 m	Rigid platform
Antenna temperature T	0.1 K	0.1 K	$He^3 - He^4$ dilution refrigerator
Platform temperature T_{pl}	0.1 K	4.2 K	Large cryogenic chamber and cooling system
Platform quality factor Q_{pl}	10^6	10^7	Al platform structure
DM frequency f_D	0.01 Hz	0.01 Hz	Magnetic levitation (horizontal only)
DM quality factor Q_D	10^8	10^8	Surface polished pure Nb
Pump frequency f_p	50 kHz	50 kHz	Tuned capacitor bridge transducer
Amplifier noise no. n	5	2	Two-stage dc SQUID
Detector noise $S_h^{1/2}(f)$	8×10^{-19} Hz$^{-1/2}$	4.5×10^{-21} Hz$^{-1/2}$	Best sensitivity at 1Hz

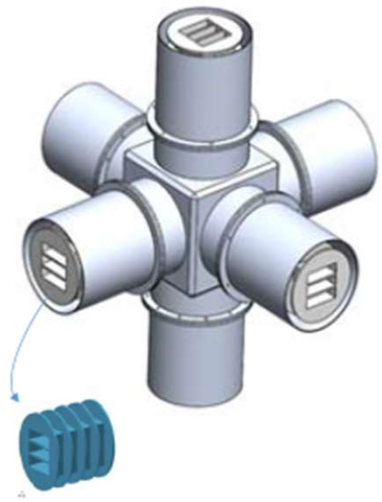

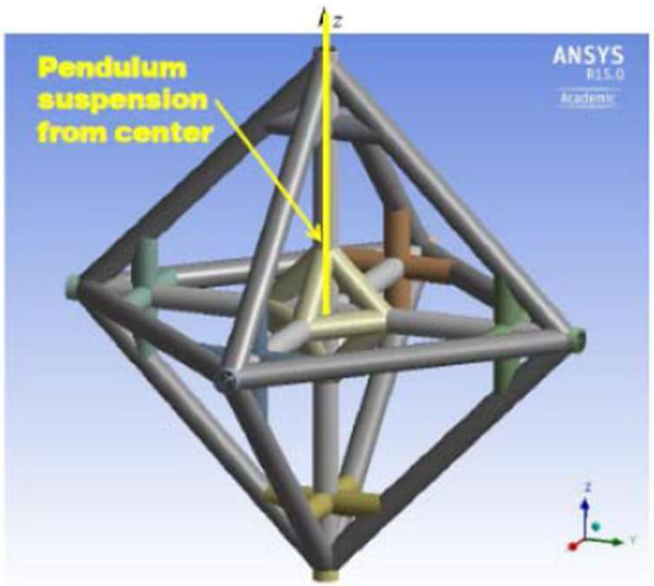

✓ Detector sensitivity and source strengths:

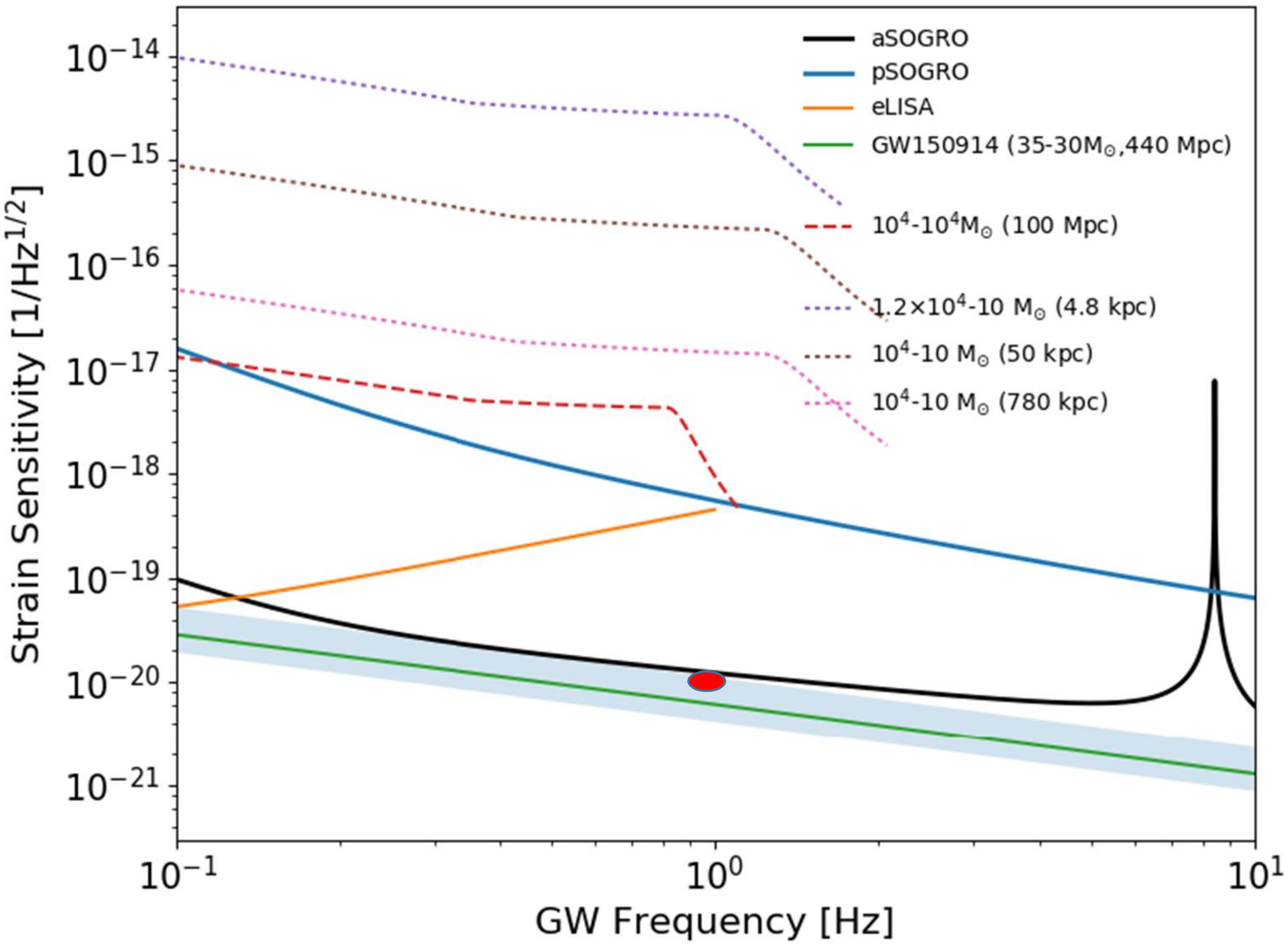

$$f_{ISCO,GW} = \frac{1}{\pi}\left(\frac{1}{6}\right)^{1.5}\frac{c^3}{GM} \sim \frac{4396}{M/M_\odot}\ [\mathrm{Hz}]$$

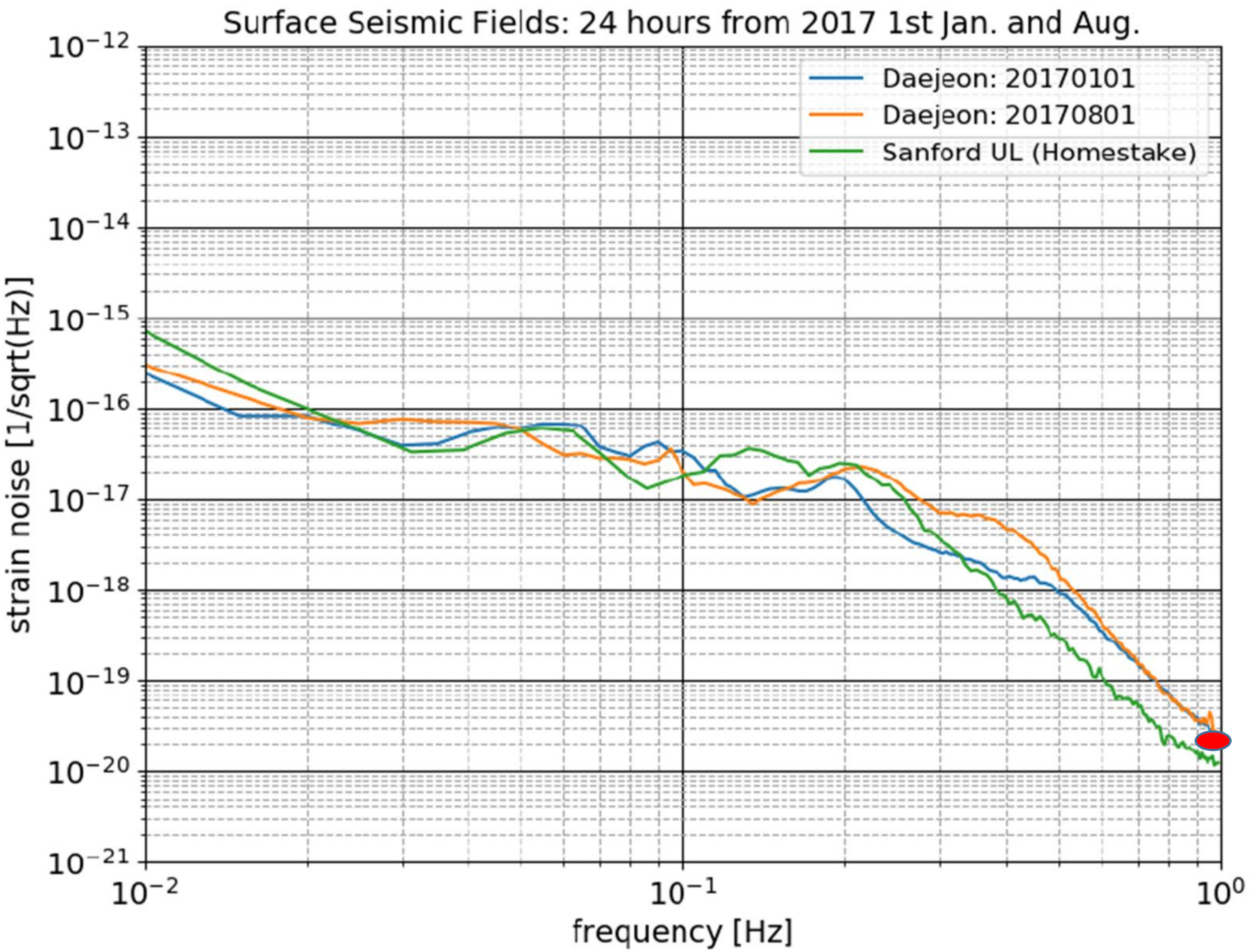
Surface Seismic Fields: 24 hours from 2017 1st Jan. and Aug.
10^{-12}
10^{-13}
10^{-14}
10^{-15}
10^{-16}
10^{-17}
10^{-18}
10^{-19}
10^{-20}
10^{-21}
strain noise [1/sqrt(Hz)]
10^{-2}
10^{-1}
10^{0}
frequency [Hz]
Daejeon: 20170101
Daejeon: 20170801
Sanford UL (Homestake)

2. Targets and Science

1) Inspiralling BBH:

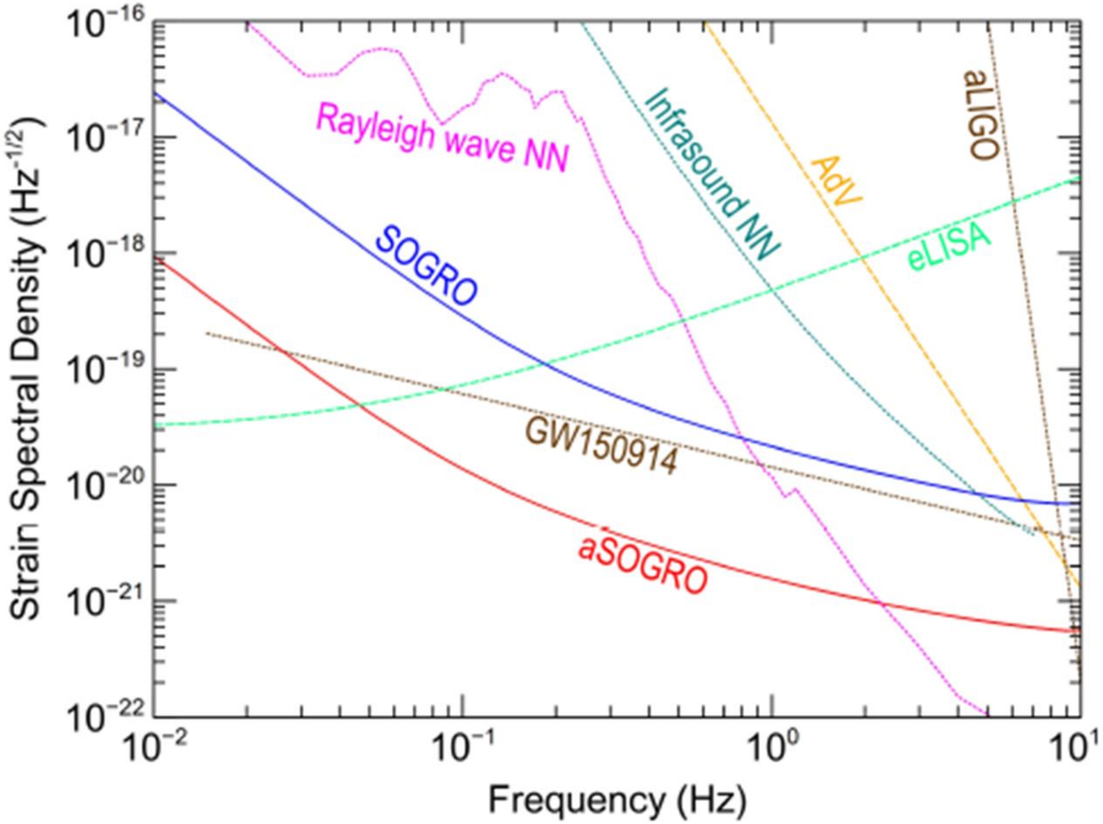

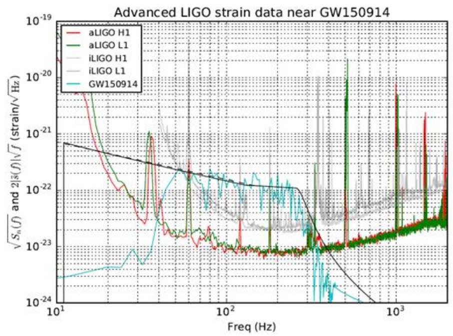

~ 10 days

Observed for ~.2s

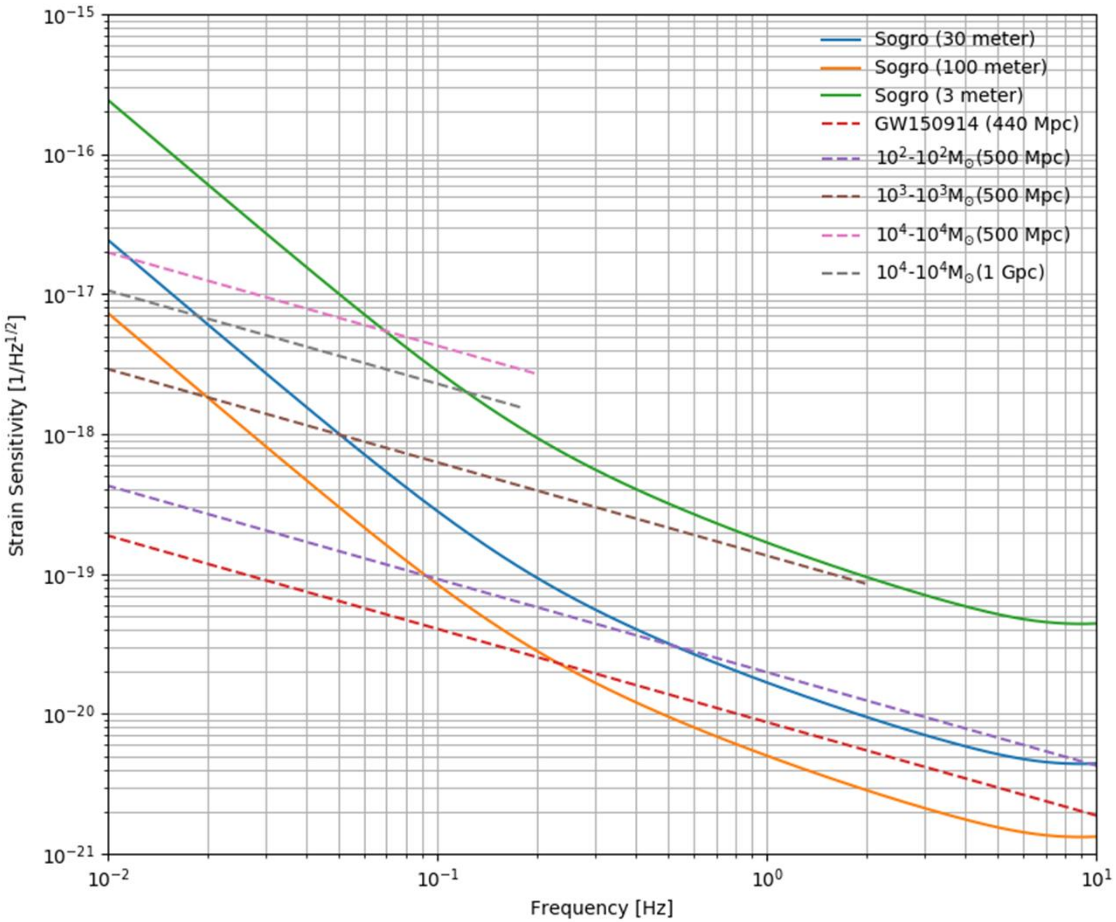


```
Mt   = 5e3           # the mass of each test mass
L0   = 3e1           # the arm length
Tt   = 1.5           # the temperature of the test mass
Mp   = {...}         # the effective mass of the platform (DM modes obtained by Ansys analysis)
Tp   = 1.5           # the temperature of the platform
C    = 4e-9          # the equilibrium capacitance of each sensing capacitor
Ep   = 5e5           # the amplitude of the driving electric field at wp
Qp   = 1e6           # the electrical quality factor
fp   = 5e4           # the pump frequency
fD   = 0.01          # the DM resonance frequency
QD   = 5e8           # the DM quality factor
n0   = 20            # Amplifier noise number
hbar = 1.05457e-34   # Planck constant
kB   = 1.38065e-23   # Boltzmann constant
Q    = 5e6           # the quality factor of the platform
f0   = {...}         # the resonance frequency of the platform (DM modes obtained by Ansys analysis)
```

	observation time	SNR
GW150914 (440 Mpc) (0.23-10 Hz)	~1.2 day (100m Sogro)	~2.3
10^2-10^2 M$_\odot$ (500 Mpc) (0.5-10 Hz)	~0.5 hr (30m Sogro)	~1.5
10^3-10^3 M$_\odot$ (500 Mpc) (0.05-2 Hz)	~5.6 hr (30m Sogro)	~7.9
10^4-10^4 M$_\odot$ (500 Mpc) (0.01-0.2 Hz)	~6.0 hr (30m Sogro)	~15
10^4-10^4 M$_\odot$ (1 Gpc) (0.02-0.18 Hz)	~1.5 hr (30m Sogro)	~7.2

100m Sogro : L0 = 1.e2, 3m Sogro: L0=3.e0
Platform thermal Sxi is included.

GW150914 (spin-precessing waveform model, arXiv:1606.01210)
Mass: 35M$_\odot$-30M$_\odot$
Luminosity distance: 440 Mpc

Slide credit: Y.-B. Bae

2) IMBH binary inspirals and mergers:

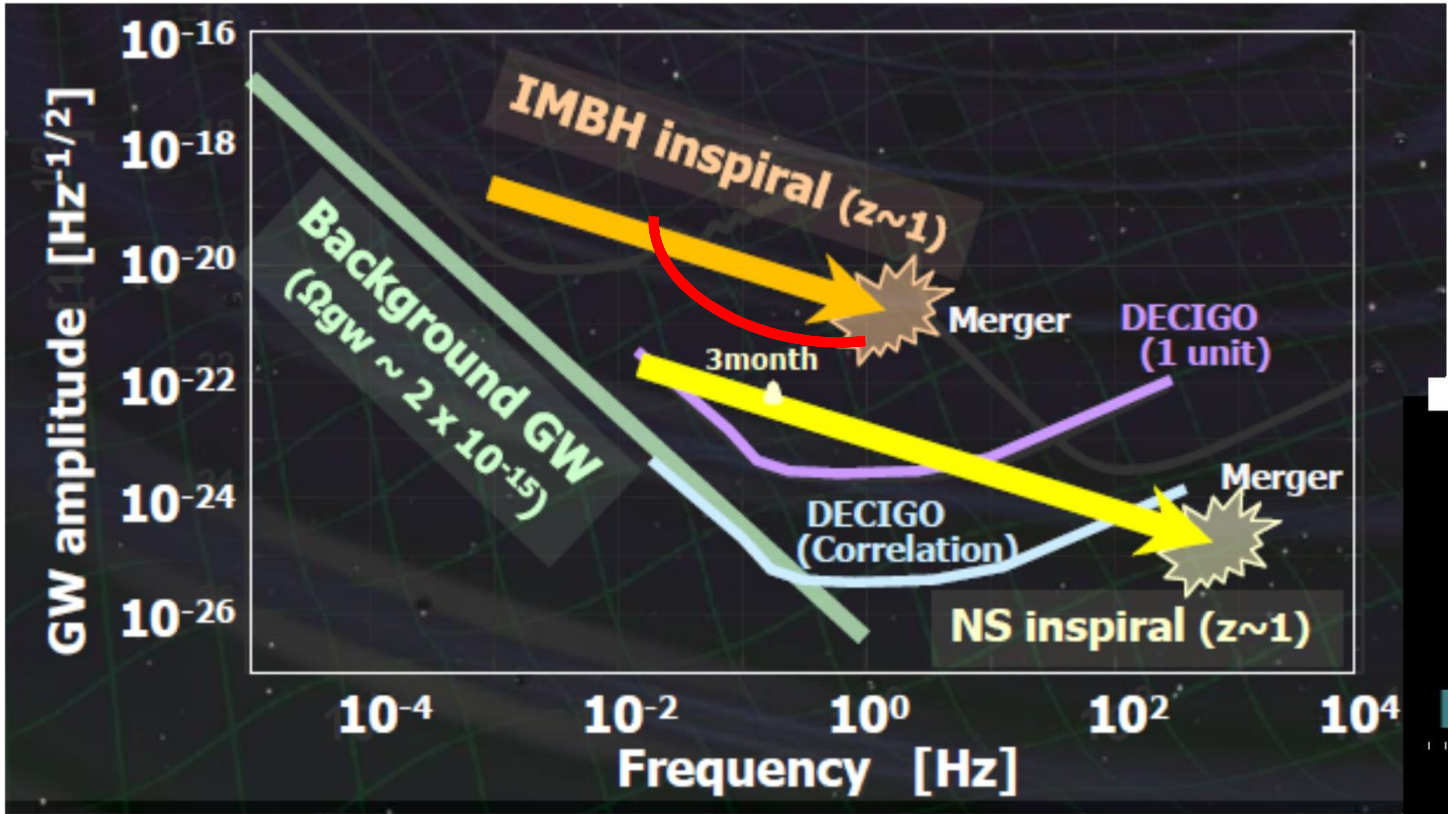

(Figure credit: M. Ando '12)

(Figure credit: C. Kim '17)

예측	최소 기준값	기준값	최대 기준값
조 건 $R_{double}/R_{single} = 1.5$	, , , 년, 임의의 공전 면 방향		
	$M_\odot$, ,	$M_\odot$, , ,	$M_\odot$, , ,
Event rate (yr^{-1})	7.6×10^{-3}	0.41	4.8

✓ X. Chen & P. Amaro-Seoane ('17):

"Formation of stellar-mass binary black holes"

Binary star evolution

vs

Dynamical interactions in dense stellar systems

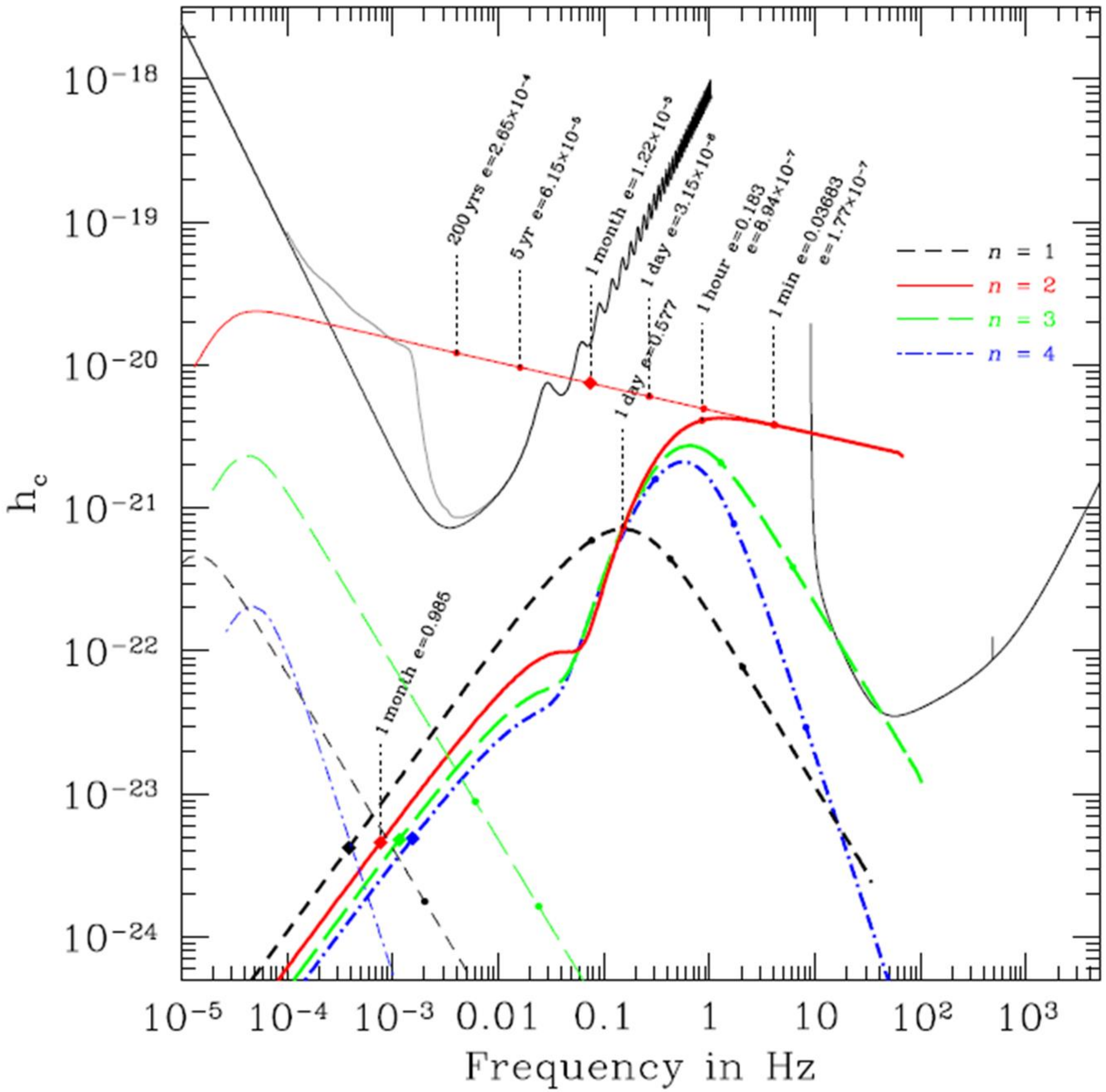

3) Stochastic Gravitational Wave Background: C. Park ('17)

$$\Omega_{GW}(f) \equiv \frac{f}{\rho_c}\frac{d\rho_{GW}}{df}$$

$$S_{\rm gw}(f) = \frac{3H_0^2}{10\pi^2}\, f^{-3}\Omega_{\rm gw}(f)$$

$$h(f) = S_{\rm gw}^{1/2}(f) = 5.6\times10^{-22}\, h_{100}\sqrt{\Omega_0}\left(\frac{100{\rm Hz}}{f}\right)^{3/2} {\rm Hz}^{1/2}$$

$$[\Omega_{gw}(f)]_{min} = \frac{\pi^2}{3H_0^2} f^3 S_n(f) [S/N]^2_{min}$$

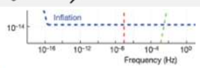

$$\simeq 1.5\times10^{-3}\left(\frac{f}{1Hz}\right)^3\left(\frac{\sqrt{S_n(f)}}{10^{-20}Hz^{-1/2}}\right)^2\left(\frac{[S/N]_{min}}{5}\right)^2$$

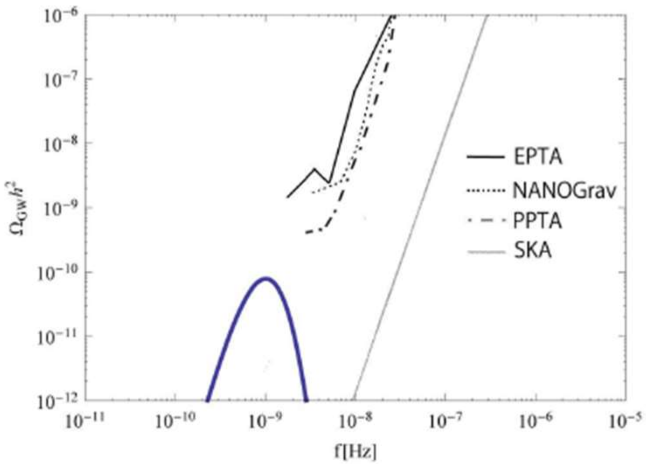

Cheng, Lee & Ng ('17)

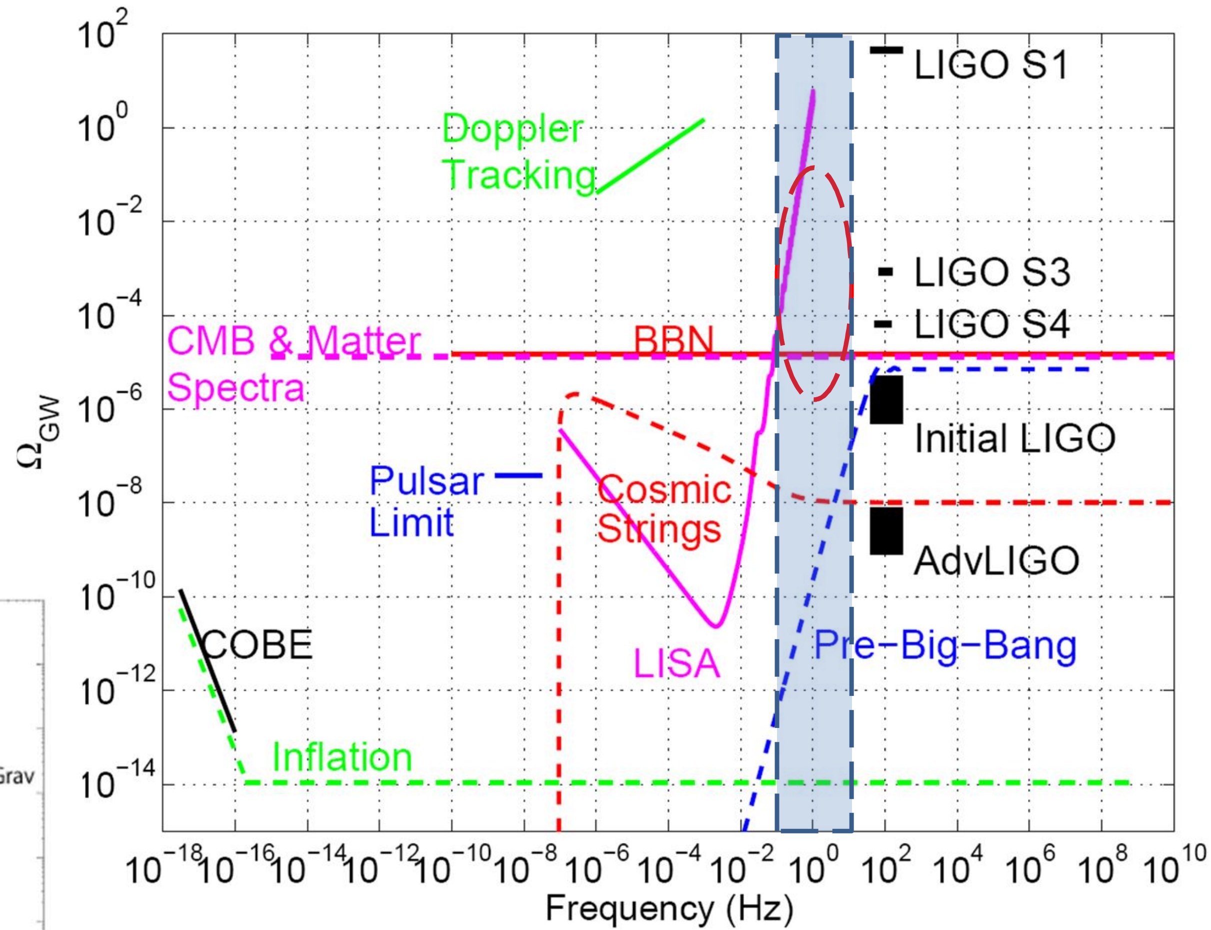

(Figure credit: G. Gonzalez '08)

✓ Build multi detectors!: Chan's talk

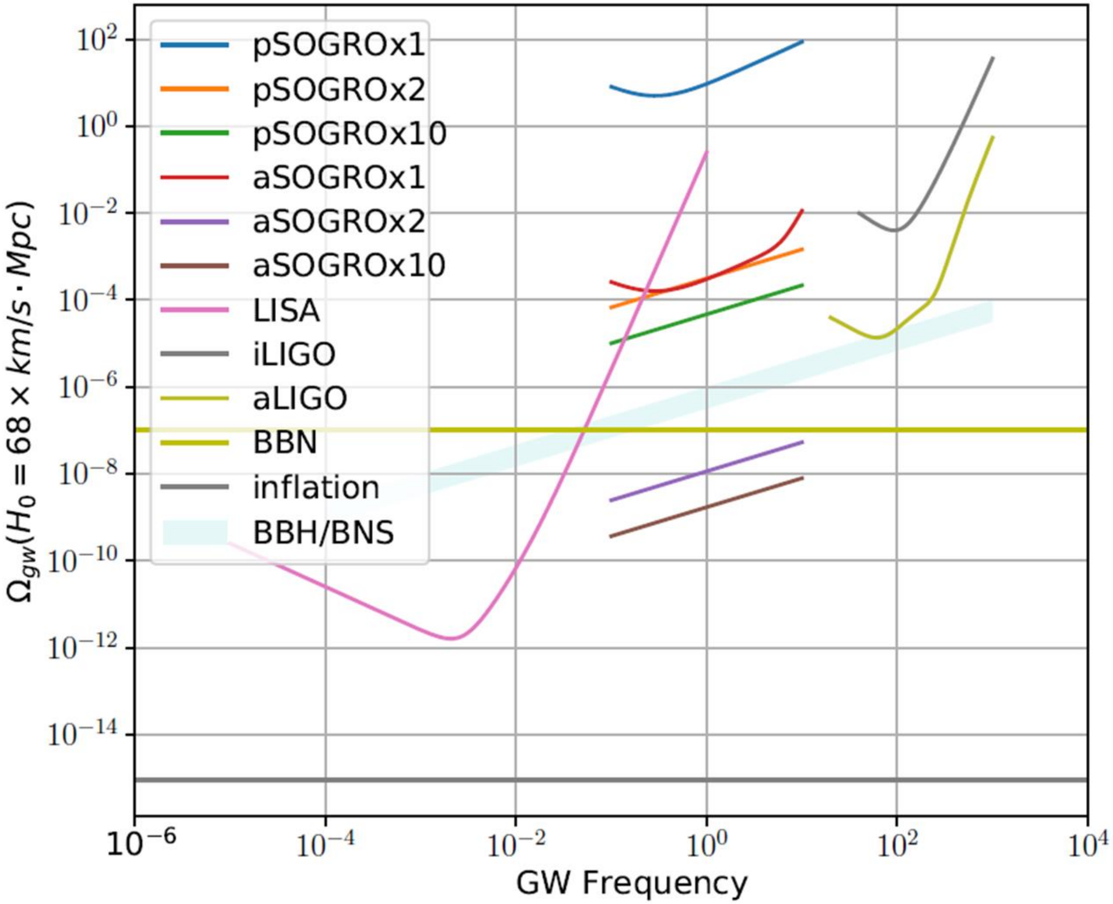

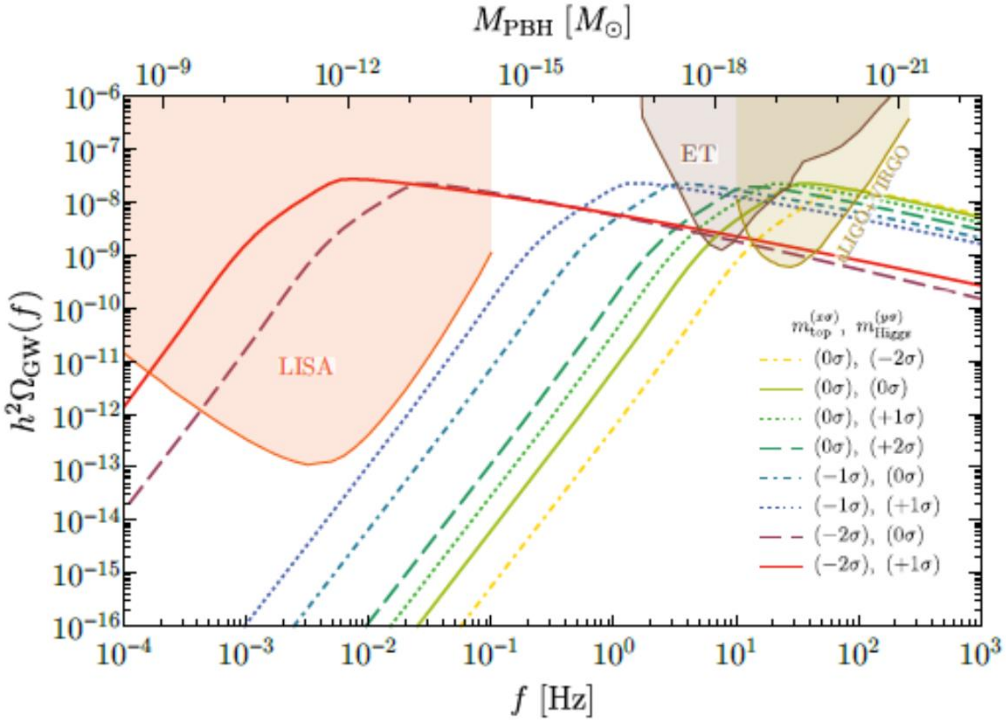

✓ Espinosa, Racco & Riotto ('18): "SM Higgs instability"

4) Other applications:

Earthquake Early Warning

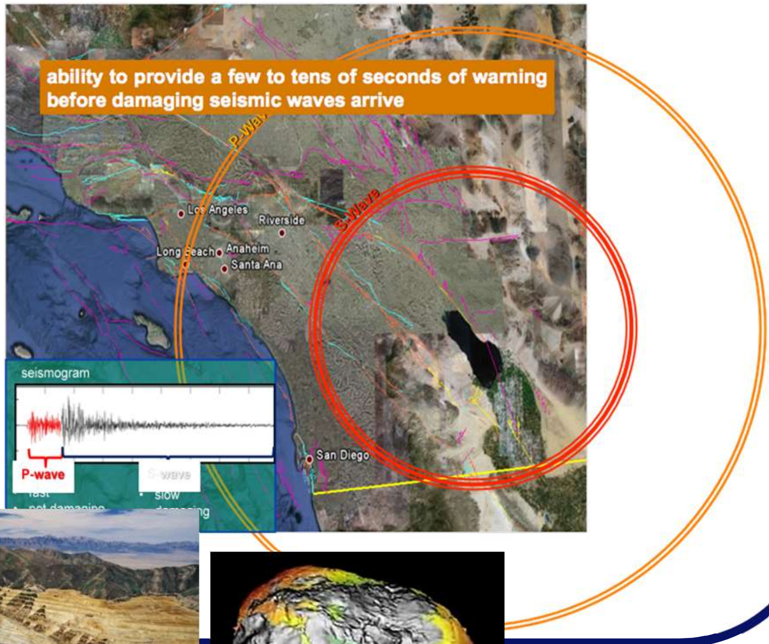

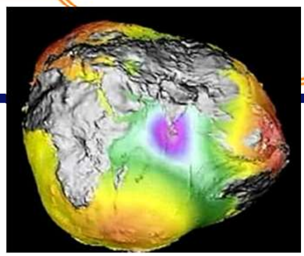

Improve aLIGO sensitivity at low freqs.

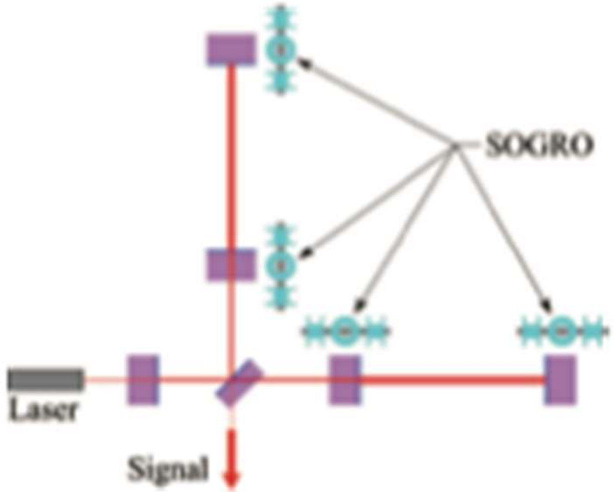

(Figure credit: C. Kim '17)

3. Concept for Cooling SOGRO System – 2nd Stage : 0.1 K

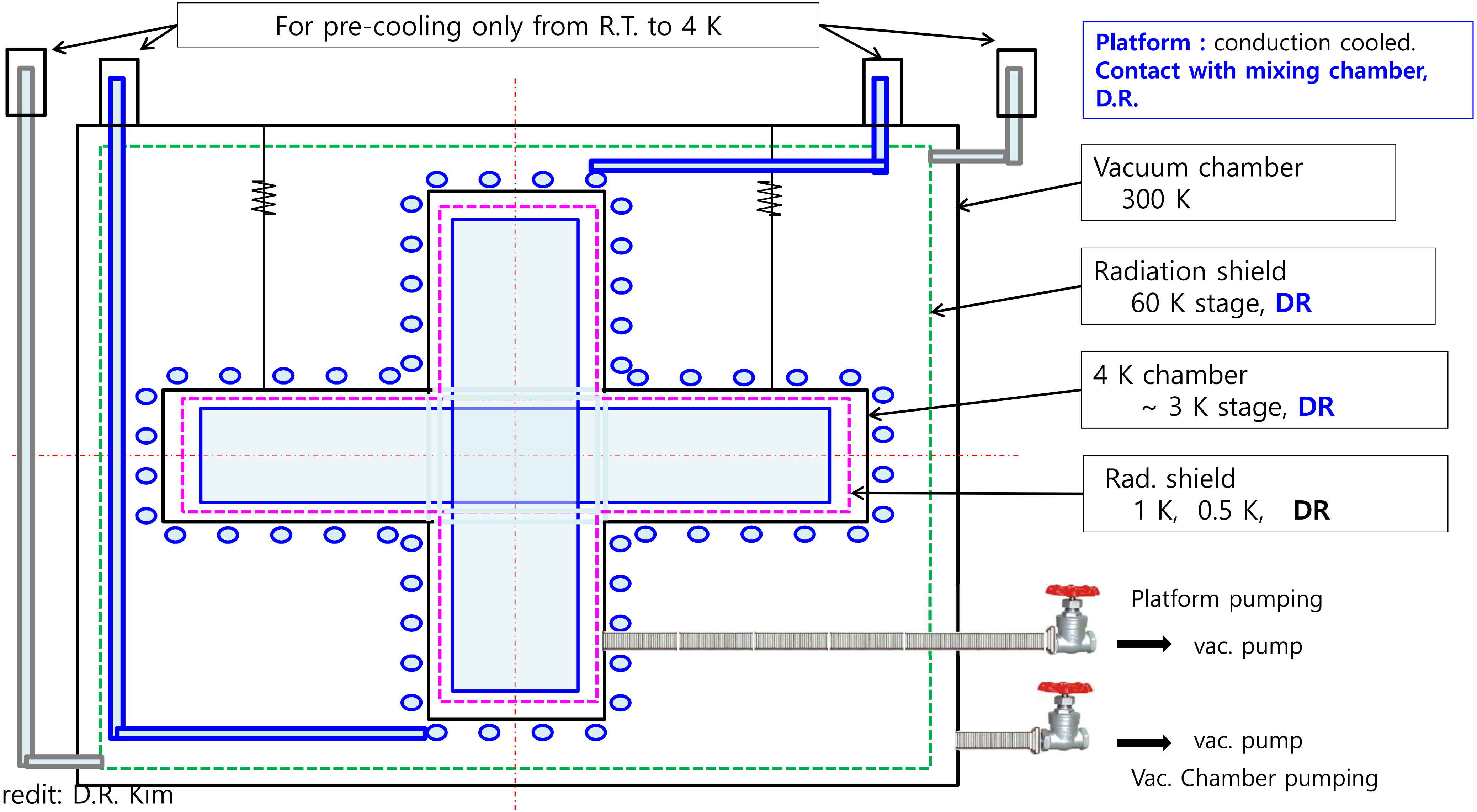

Slide credit: D.R. Kim

4. Budget estimated

- ✓ pSOGRO: ~30 million dollars in total for 6 years

- ✓ aSOGRO: ?? but ~10 times more……

V. Summary

- Current status of GW detections and perspectives are summarized.
- Design, principles, sciences and challenges are briefly introduced for the project of developing a superconducting mid-frequency gravitational wave telescope (SOGRO).
- We do not know as yet if this project will be successful although we are doing our best for it.

- But, we strongly believe that it will bring lots of fruitful sciences and new chances in the future.
- Lots of interest, support and active participation of other people in various fields are essential.

- **International collaborations are highly desirable**, for instance, in multi detector stochastic GW background observations.

1/10^(-21) OF THANKS!

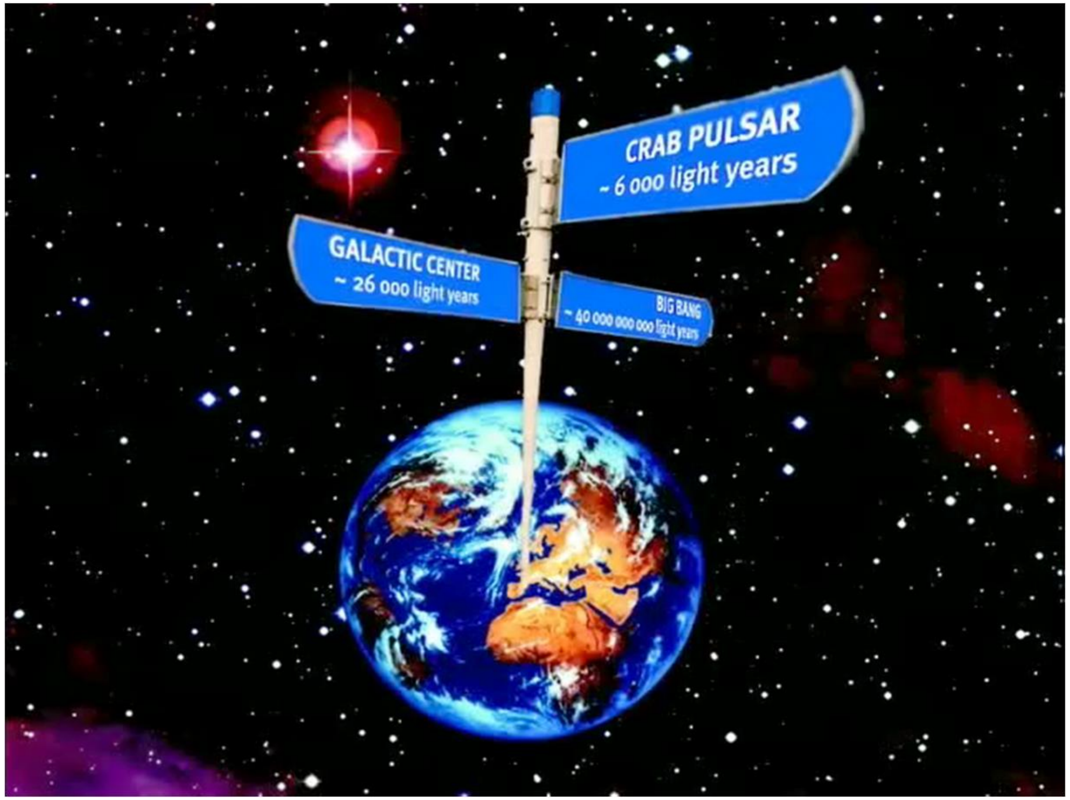

Sources of Noises

- Laser shot noise
  - Inrcrease laser power, resonant cavity, power recycling
- Radiation pressure noise
  - Make mirrors heavierSuspension thermal noise/ mirror coating brownian noise
  - Increase beam size, monolithic suspension structure
- Seismic noise
  - Multi-stage suspension, underground
- Newtonian Noise
  - So far difficult to avoid. Seismic and wind measurement and careful modeling

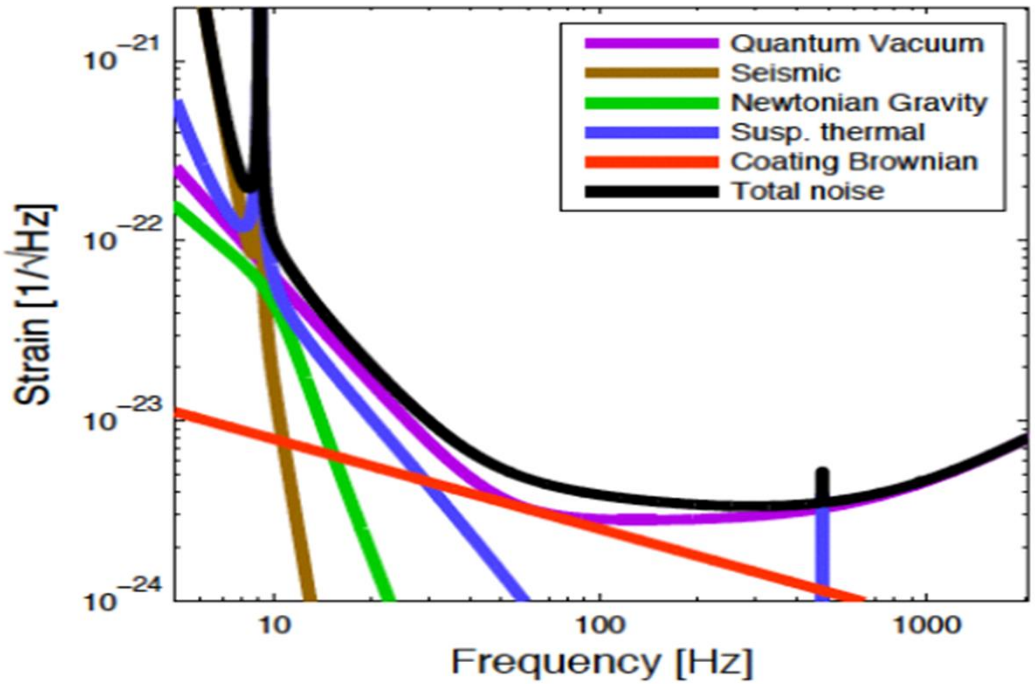

Antenna pattern

LIGO

× polarization

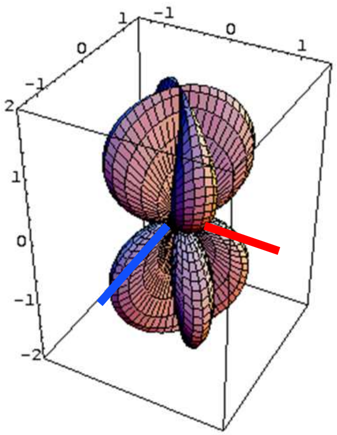

+ polarization

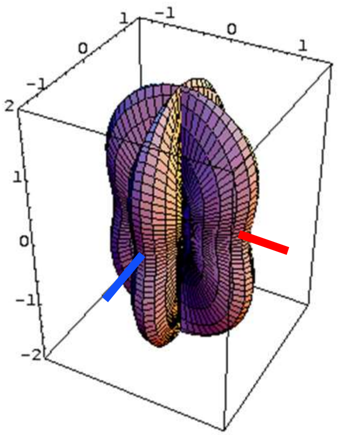

rms sensitivity

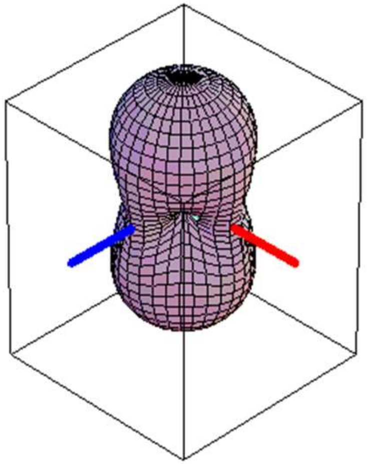

Sky location of GW150914

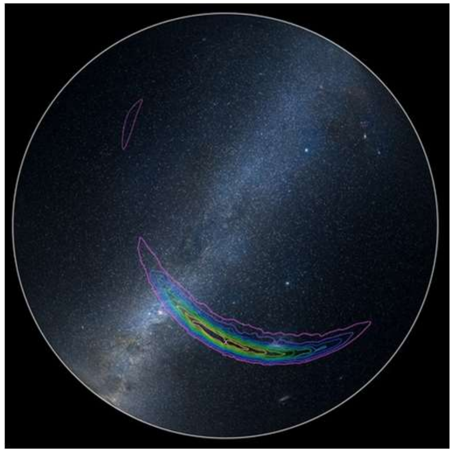

SOGRO

Diagonal

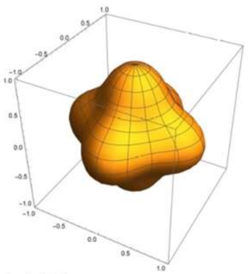

Off-diagonal

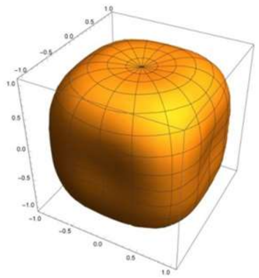

Total

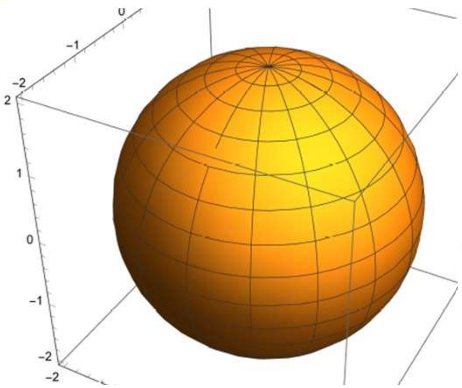

Sky location by SOGRO

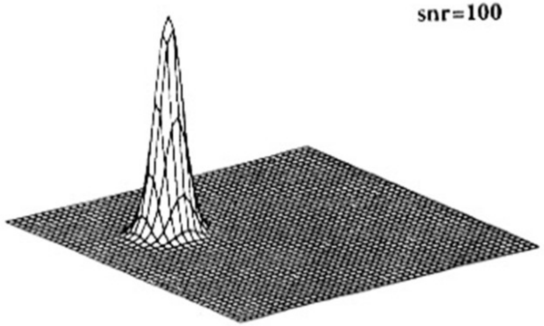

(Slide credit: Paik ’16)

Main Noises

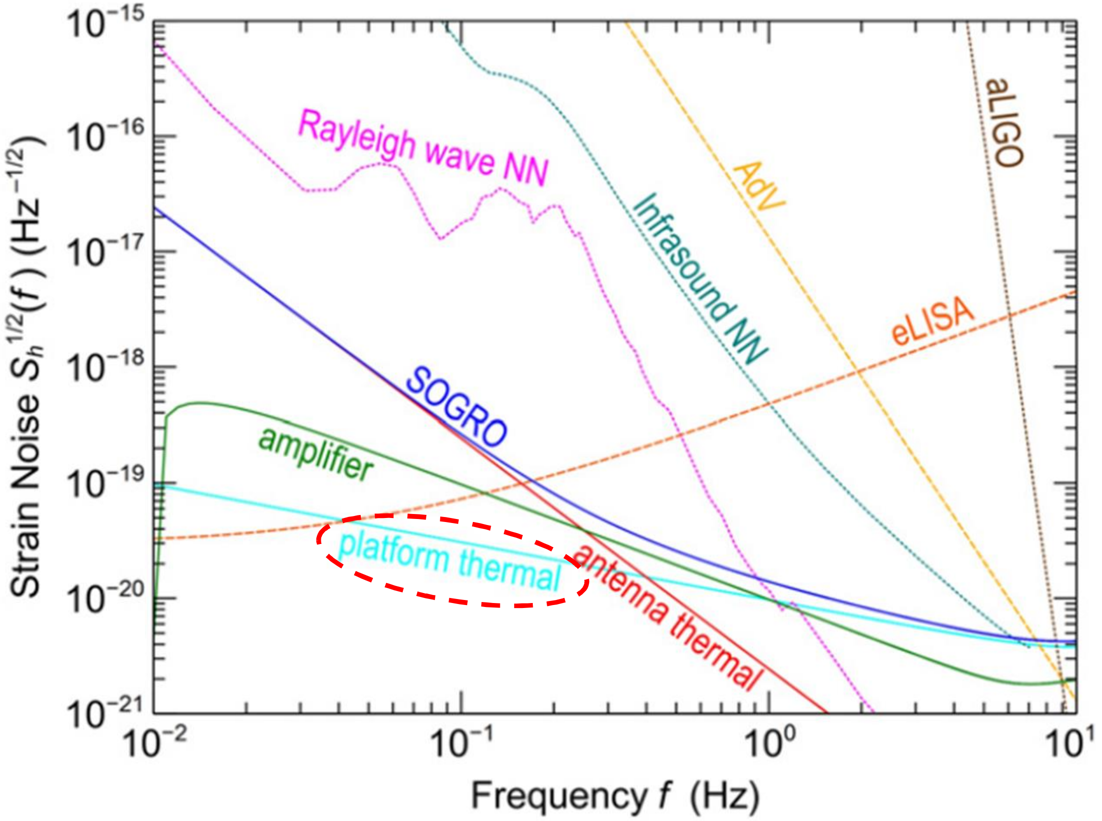

- Understanding its characteristic features is essential for designing the whole experiments.
- Goal: Find out the optimal design(s) for the platform which satisfies (all) desired requirements.

- So, we have investigated the thermal noise features of various SOGRO platforms, and report some preliminary results.

XY-Mode No.	Freqs. (Hz)	KE (10^4J)	dx (10^{-3}m)	m_{eff} (10^3 kg)
11	8.4306	0.140	2.0832	229.943
40	23.203	1.06	1.46682	463.590
65	31.575	1.97	5.5071	33.0068
68	32.662	2.11	12.158	6.77864
83	46.566	4.28	0.44362	5081.06

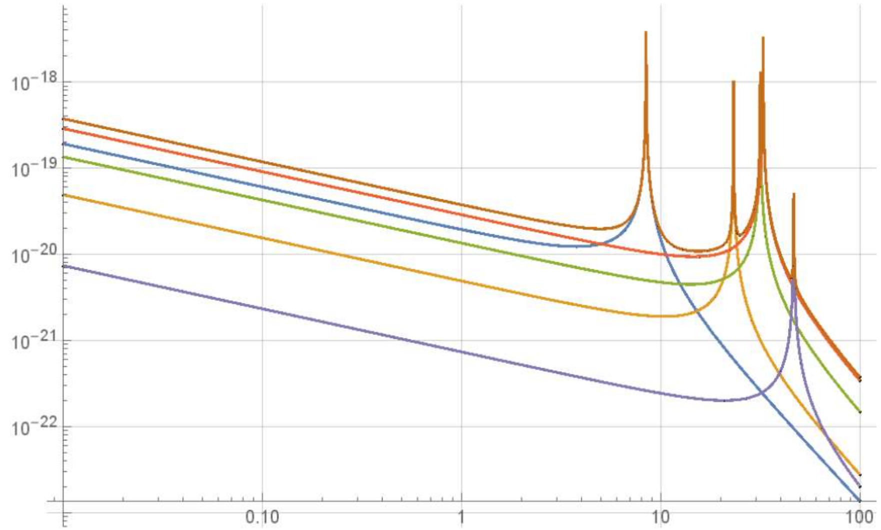

Thermal strain noise for first 5 XY modes and total: 50-m

XX-Mode No.	Freqs. (Hz)	KE (10^6J)	dx (10^{-2}m)	m_{eff} (kg)	$\frac{2KE}{\delta x^2}$ (10^6)
34	626.69	7.75	3.81	688.678	
35	626.69	7.75	14.333	48.6623	
72	1880.1	69.8	8.7981	129.237	
73	1880.1	69.8	11.939	70.1823	
136	3135.5	69.8	4.9473	146.952	
137	3135.5	69.8	13.982	18.3981	
XY-Mode No.	Freqs. (Hz)	KE (10^5J)	dx (10^{-2}m)	m_{eff} (kg)	$\frac{2KE}{\delta x^2}$ (10^6)
7	102.58	2.08	9.6118	108.392	
27	463.89	2.08	11.552	3.66935	

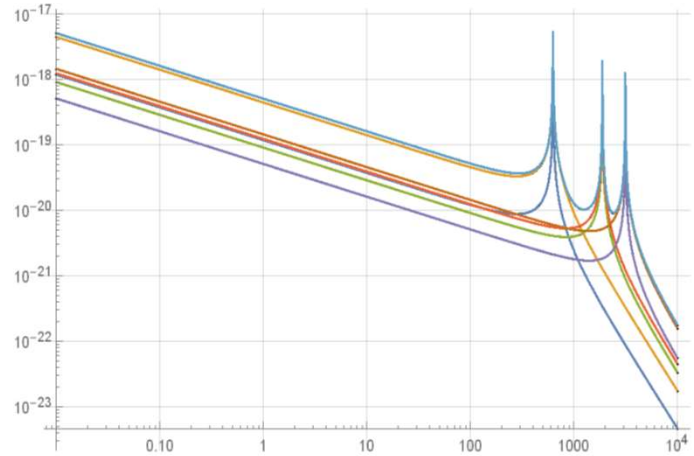

Thermal strain noise for first 5 XX modes and total: 2-m

Newtonian gravity noise

- Seismic and atmospheric density fluctuations produce NN.
- GWs are transverse whereas near-field Newtonian gradient is not.
  ⇨ Could GW signal be separated out from NN?

In the GW coordinate system,

$$h'(\omega) = \begin{pmatrix} h_+(\omega) + h'_{N11}(\omega) & h_\times(\omega) + h'_{N12}(\omega) & h'_{N13}(\omega) \\ h_\times(\omega) + h'_{N12}(\omega) & -h_+(\omega) + h'_{N22}(\omega) & h'_{N23}(\omega) \\ h'_{N13}(\omega) & h'_{N23}(\omega) & h'_{N33}(\omega) \end{pmatrix}, \text{ where}$$

$$h'_{N11}(\omega) = \sum_i \left[a(\omega)\xi_i(\omega) + b(\omega,\vartheta_i)\delta\rho_i(\omega)\right]\left[\cos(\psi_i - \phi)\cos\theta + i\sin\theta\right]^2$$

$$h'_{N22}(\omega) = \sum_i \left[a(\omega)\xi_i(\omega) + b(\omega,\vartheta_i)\delta\rho_i(\omega)\right]\sin^2(\psi_i - \phi)$$

$$h'_{N33}(\omega) = \sum_i \left[a(\omega)\xi_i(\omega) + b(\omega,\vartheta_i)\delta\rho_i(\omega)\right]\left[\cos(\psi_i - \phi)\sin\theta - i\cos\theta\right]^2$$

$$h'_{N12}(\omega) = \sum_i \left[a(\omega)\xi_i(\omega) + b(\omega,\vartheta_i)\delta\rho_i(\omega)\right]\sin(\psi_i - \phi)\left[\cos(\psi_i - \phi)\cos\theta + i\sin\theta\right]$$

$$h'_{N23}(\omega) = \sum_i \left[a(\omega)\xi_i(\omega) + b(\omega,\vartheta_i)\delta\rho_i(\omega)\right]\sin(\psi_i - \phi)\left[\cos(\psi_i - \phi)\sin\theta - i\cos\theta\right]$$

$$h'_{N13}(\omega) = \sum_i \left[a(\omega)\xi_i(\omega) + b(\omega,\vartheta_i)\rho_i(\omega)\right]\left[\cos(\psi_i - \phi)\cos\theta + i\sin\theta\right]\left[\cos(\psi_i - \phi)\sin\theta - i\cos\theta\right]$$

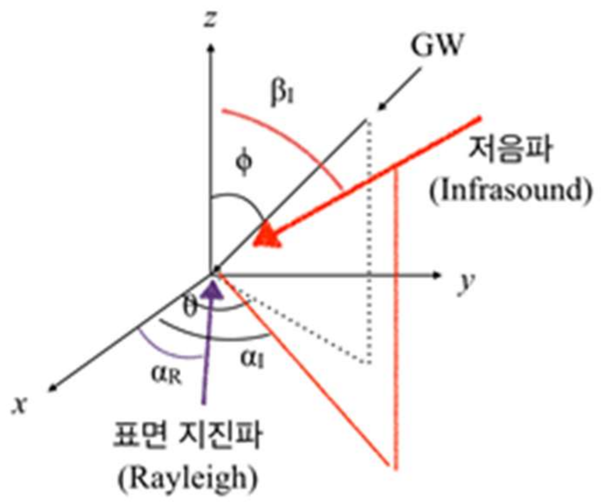

(Figure Credit: H-M. Lee '17)

- Tensor measurement is insufficient to remove NN from multiple waves.
  ⇨ Still requires external seismometers and microphones.

(Credit: Paik '16)

Extraction of GWs: Harms & Paik PRD ('16)

$$h_+ = h'_{11} - 2\cot(\theta)h'_{13} + \cot^2(\theta)h'_{33}$$

$$+ \csc^2(\theta)2\pi\gamma G\rho_0 \frac{k}{\omega^2}\sum_i \xi_i(\omega),$$ ➔ Effect due to Rayleigh-wave

$$+ \csc^2(\theta)\frac{4\pi}{\omega^2}\frac{G\rho_0}{\gamma p_0}\sum_i \delta p_i(\omega)\sin^2(\beta_i)$$ ➔ Effect due to Infrasound-wave

$$h_\times = h'_{12} - \cot(\theta)h'_{23}$$

$$+ \mathrm{i}\csc(\theta)2\pi\gamma G\rho_0 \frac{k}{\omega^2}\sum_i \xi_i(\omega)\sin(\alpha_i - \phi)$$ ➔ Effect due to Rayleigh-wave

$$+ \mathrm{i}\csc(\theta)\frac{4\pi}{\omega^2}\frac{G\rho_0}{\gamma p_0}\sum_i \delta p_i(\omega)\sin^2(\beta_i)\sin(\alpha_i - \phi)$$ ➔ Effect due to Infrasound-wave

And use Wiener Filter ……

$$r(\omega) = 1 - \frac{\vec{C}_{\mathrm{RT}}^{\top}(\omega)\cdot(C_{\mathrm{RR}}(\omega))^{-1}\cdot\vec{C}_{\mathrm{RT}}(\omega)}{C_{\mathrm{TT}}(\omega)}.$$

Mitigation of NN

NN due to Rayleigh waves removed by using h'_{13}, h'_{23}, h'_{33}, a_z (CM), plus 7 seismometers with SNR = 10^3 at the radius of 5 km.

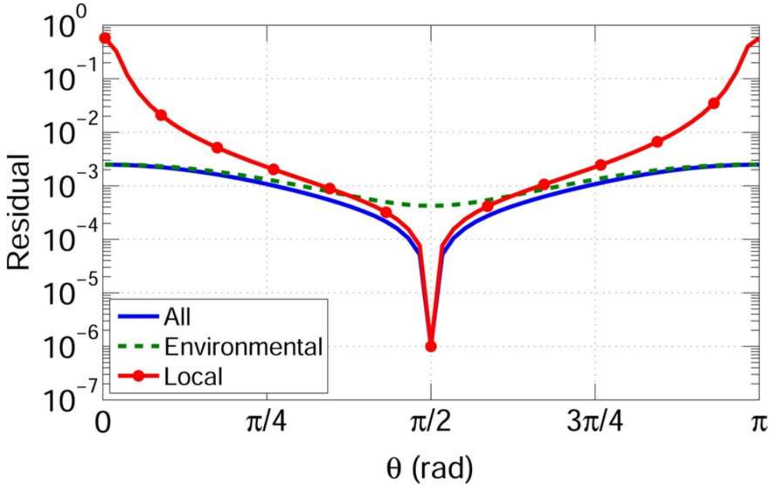

NN due to infrasound removed by using h'_{13}, h'_{23}, h'_{33} and 15 mikes of SNR = 10^4, 1 at the detector, 7 each at radius 600 m and 1 km.

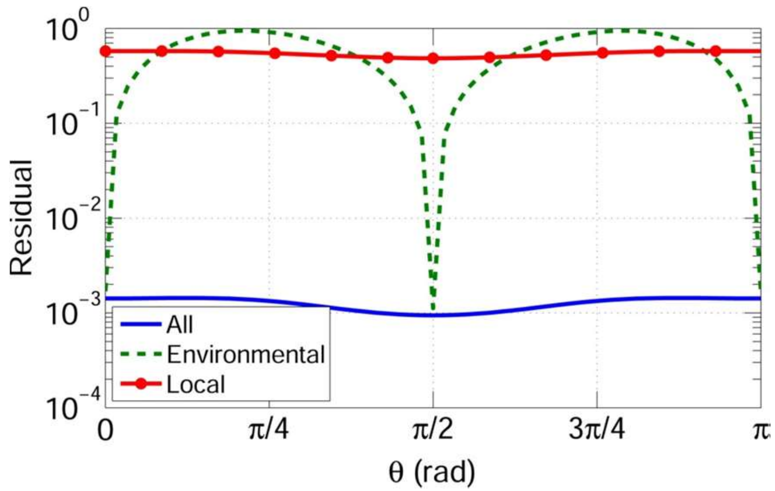

- **First remove Rayleigh NN by using seismometers only, then remove infrasound NN by using microphones and cleaned up SOGRO outputs.**
- **Unlike TOBA and laser interferometer, SOGRO can remove NN from infrasound for *all* incident angles.**

Harms and Paik, *PRD* 92, 022001 (2015)

(Slide credit: Paik ’16)